Los Alamos
NATIONAL LABORATORY
EST.1943

LA-UR-17-24021
Approved for public release; distribution is unlimited.

Title: KLYNAC: COMPACT LINEAR ACCELERATOR WITH INTEGRATED POWER SUPPLY

Author(s): Malyzhenkov, Alexander

Intended for: Master Thesis at Northern Illinois University

Issued: 2017-05-16

Disclaimer:
Los Alamos National Laboratory, an affirmative action/equal opportunity employer, is operated by the Los Alamos National Security, LLC for the National Nuclear Security Administration of the U.S. Department of Energy under contract DE-AC52-06NA25396. By approving this article, the publisher recognizes that the U.S. Government retains nonexclusive, royalty-free license to publish or reproduce the published form of this contribution, or to allow others to do so, for U.S. Government purposes. Los Alamos National Laboratory requests that the publisher identify this article as work performed under the auspices of the U.S. Department of Energy. Los Alamos National Laboratory strongly supports academic freedom and a researcher's right to publish; as an institution, however, the Laboratory does not endorse the viewpoint of a publication or guarantee its technical correctness.

ABSTRACT

KLYNAC: COMPACT LINEAR ACCELERATOR WITH INTEGRATED POWER SUPPLY

A. V. Malyzhenkov, M.S.
Department of Physics
Northern Illinois University, 2017
Philippe Piot, Director

Accelerators and accelerator-based light sources have a wide range of applications in science, engineering technology and medicine. Today the scientific community is working towards improving the quality of the accelerated beam and its parameters while trying to develop technology for reducing accelerator size. This work describes a design of a compact linear accelerator (linac) prototype, resonant Klynac device, which is a combined linear accelerator and its power supply - klystron. The intended purpose of a Klynac device is to provide a compact and inexpensive alternative to a conventional 1 to 6 MeV accelerator, which typically requires a separate RF source, an accelerator itself and all the associated hardware. Because the Klynac is a single structure, it has the potential to be much less sensitive to temperature variations than a system with separate klystron and linac. We start by introducing a simplified theoretical model for a Klynac device. We then demonstrate how a prototype is designed step-by-step using particle-in-cell simulation studies for mono-resonant and bi-resonant structures. Finally, we discuss design options from a stability point of view and required input power as well as behavior of competing modes for the actual built device.

NORTHERN ILLINOIS UNIVERSITY
DE KALB, ILLINOIS

MAY 2017

KLYNAC: COMPACT LINEAR ACCELERATOR WITH INTEGRATED POWER SUPPLY

BY

A. V. MALYZHENKOV
© 2017 A. V. Malyzhenkov

A THESIS SUBMITTED TO THE GRADUATE SCHOOL

IN PARTIAL FULFILLMENT OF THE REQUIREMENTS

FOR THE DEGREE

MASTER OF SCIENCE

DEPARTMENT OF PHYSICS

Thesis Director:
Philippe Piot

ACKNOWLEDGEMENTS

I would like to thank the United States Department of Energy Laboratory Directed Research and Development (LDRD) Foundation at Los Alamos National Laboratory (LANL) for financial support of the project; Dr. Bruce Carlsten for invitation to the project, computer simulation code, and active scientific discussions; Dr. James Potter for designing the actual structure in 3D; Dr. Kimberley Nichols for finishing the design and leading the production and experimental part of the project; Dr. Greg Dale and Dr. Dale Dalmas for setting up the experimental setup and solving a lot of technical issues; Dr. Dmitry Shchegolkov for providing safety help for the experiment and engineering discussions; and Dr. Petr Anisimov and Dr. Alexander Scheinker for active scientific discussions and nonstandard view on the problem. Finally, I would like to thank Dr. Alexander Scheinker one more time for proofreading this manuscript.

DEDICATION

To my loving friends and family, to the Pacific Ocean and never-ending waves on the Hawaiian shore...

TABLE OF CONTENTS

LIST OF FIGURES

Figure Page

Figure Page

CHAPTER 1

INTRODUCTION

1.1 The Klynac concept

Accelerators and accelerator-based light sources have a wide range of applications in science, engineering technology and medicine. Today, the scientific community is working towards improving the quality of the accelerated beams while trying to develop technology for reducing accelerator footprint. A more compact accelerator will significantly increase application capability, reduce cost, and result in a wide dissemination of these systems.

An accelerator system consists of an accelerator, power supplies, radio frequency (RF) power generators (klystron), feedback control system, stabilization system and possibly a cryogenic system in the superconducting case. Therefore, one may combine the various components to reduce the overall size. Due to the similar structure and physical principles of an accelerator and a klystron, it was suggested to combine them into one single structure (Fig. 1.1). In such a device the electron beam emitted from an electron gun will first travel through the klystron sections transferring its energy to the RF field and slowing down. The beam is then collimated through the aperture, which allows only the small fraction of the electron beam to go through to the accelerator section. The resulting low-charge electron bunch is then accelerated by the RF field. Thus, this fraction of the electron bunch gets the energy from the initial bunch emitted from the electron gun. In addition, the combination of klystron and accelerator in a single structure will automatically maintain a common frequency among its parts, independent of temperature drift and other instabilities, which

potentially allows one to avoid using a feedback system to keep the accelerator on resonance with the klystron output.

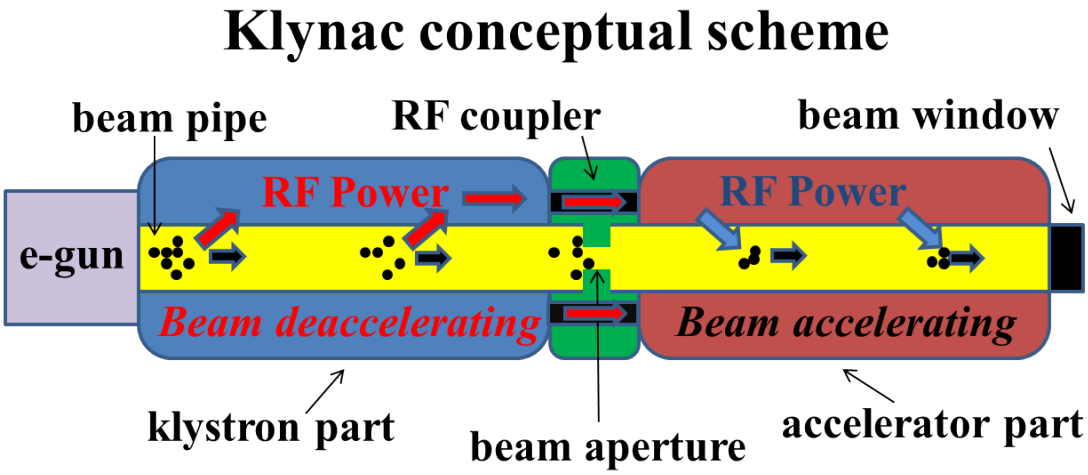

Figure 1.1: Klynac simplified scheme.

There is another way to understand the new physics of a Klynac device by looking at it in a more general way. Imagine the electron beam with some initial average energy enters a "black-box" accelerator. Inside of the machine some interesting process is going on. The average energy of the beam is transfered to a small fraction of the beam. At the exit, only the accelerated fraction of the beam is of particular interest. Meanwhile, a large part of the beam with a smaller energy is blocked or damped. The potential description of what is happening inside of such a black box accelerator is an interaction between different particles and the structure. This type of interaction is a nonlinear process. Energy is transfered from one particle to another via interaction with a resonant structure, building up power from initial noise or a lower power input signal. Typically the interactions of the particles within beam are called collective effects [1]. In the early days collective methods had been proposed for particle acceleration [2]. Today acceleration of a small beam driven by a wake field produced by another big beam is actively discussed [3]. Klynac, in some sense, can

be assumed as a device where larger part of a beam accelerates smaller part of the same beam. We would like to add that the generalized Klynac type of a device is not specifically a combination of a klystron and an accelerator, but a device where the small fraction of the beam is accelerated via decelerating the rest of the beam via interaction with a structure. We finish our discussion of what a Klynac is and continue our introduction by providing an historical overview of the Klynac concept and analyzing why such a configuration was not built fifty years ago.

1.2 Klynac predecessors or the patent business

The question of what was created first, a chicken or an egg, still remains the paradigm. The question between the accelerator and the klystron is pretty well known. First, the linear accelerator was invented in 1928 by Rolf Wideroe (Fig. 1.2 left) and Leo Szilard [4, 5]. Later, in 1937, the Varian brothers, Russel and Sigurd (Fig. 1.2 right), invented and built the first klystron [6]. In 1946 Hansen and his graduate students build the 1.5 MeV electron linear accelerator Mark I driven by a 900kW magnetron. Three years later the second version, Mark II, reached the energy of 40 MeV. In 1950 the first linear accelerator driven by klystrons reached the energy of 75 MeV. Four years later John Nygard filed the patent for a compact linear accelerator, which was published in 1960. The compact linear accelerator design by John Nygard was very similar to what we propose to name Klynac today. Therefore, the first idea and one of the closest concept to the Klynac type of device was invented more than a half century ago, but from the best of our knowledge has never been built.

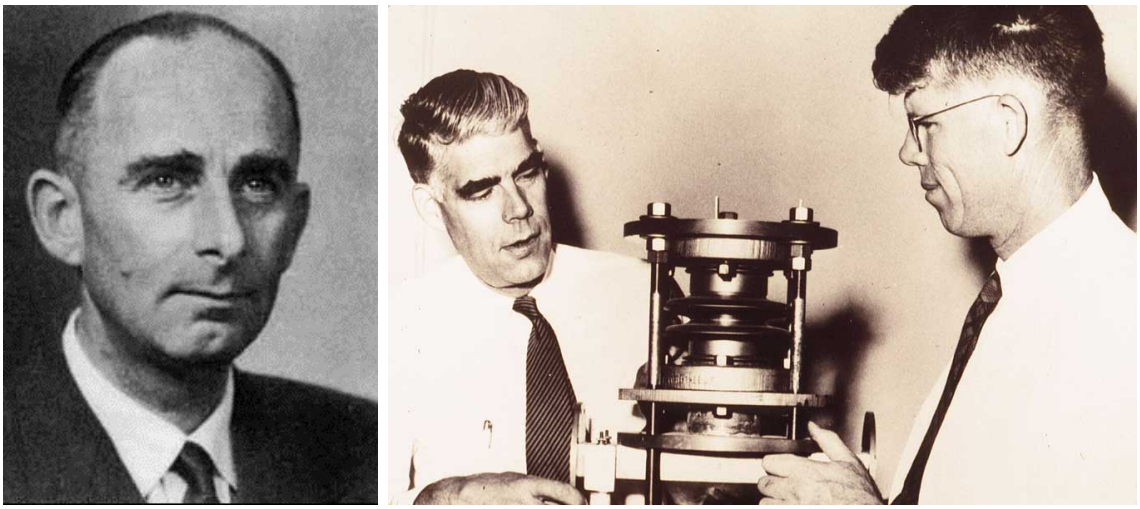

Figure 1.2: Rolf Wideroe, a pioneer of particle accelerators (left), and Varian brothers with a klystron (right).

From the patent 2,922,921 (United States Patent Office) [7]: "This invention relates to microwave linear accelerators for the acceleration electrons to high energy, and in particular to a microwave linear accelerator wherein an electron discharge device which is used to supply high frequency power to the acceleration tube or waveguide of the linear accelerator is simultaneously used to inject electrons into the waveguide, thereby eliminating the necessity for a separate electron injector."

As one can see from Fig. 1.3 and understand from the patent description, the author proposes on using one electron source, the cathode (4), for the accelerator as well as for the "electron discharge device" which he is going to realize as a klystron type of device or as a traveling wave amplifier tube. In addition, the inventor discusses the opportunity to use a magnetron as a dual-purpose electron discharge device and makes the conclusion that it does not fit in his concept, due to the magnetron not producing an electron beam. John Nygard assumes that his device may work as an oscillator, where a portion of the high-frequency power from the output resonator (16) is fed back to the input resonator (7) through the external transmission line (10). This line includes a high-Q cavity resonator

(17) to provide frequency control for a broad-band Klynac device. The rest of the output signal is transferred to the linac section through the external transmission line (3). In this line the author proposes using the phase control device so one can accelerate the fastest part of the beam entering the linac section through the aperture (20).

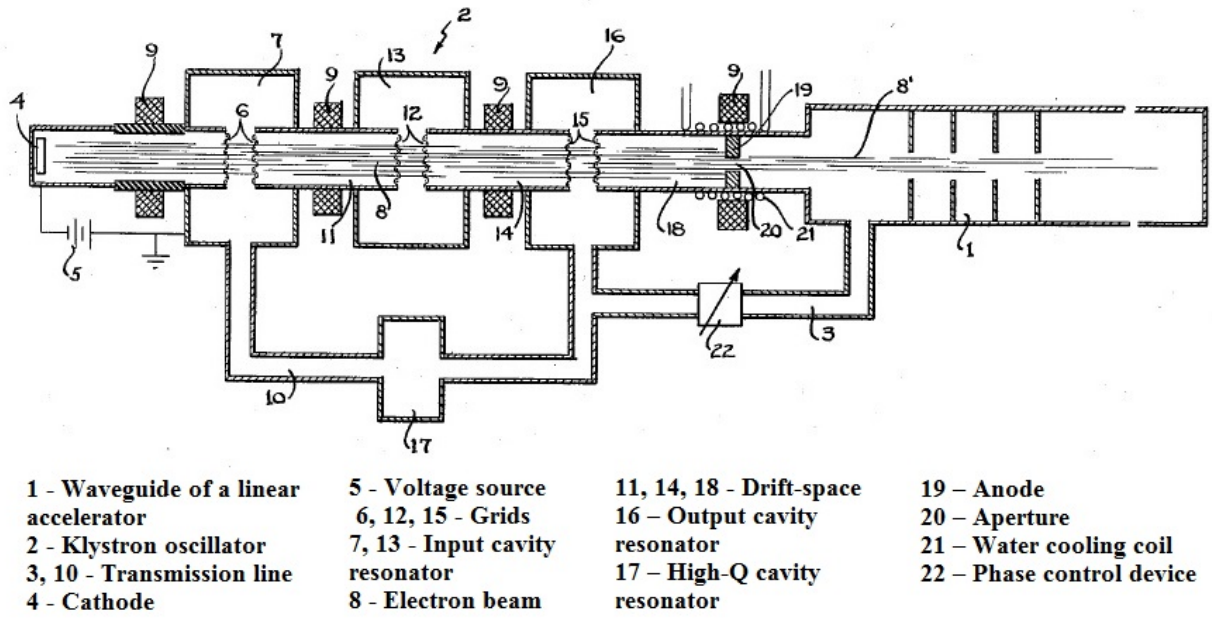

Figure 1.3: Nygard's compact accelerator scheme. Figure extracted from [7].

The inventor mitigates the risk of over-heating of the aperture (a significant part of the electron beam does not go through the aperture and heats the anode (19)) via water cooling coils (21). In addition, the author claims that the klystron (or traveling wave tube) which is used as the electron injector and power supply at the same time for the linac section need not be the high-frequency oscillator only but may also be a high-frequency amplifier of the high-frequency power supply. He adds that this power supply can be realized via using a magnetron oscillator. Summarizing the above, John **Nygard** proposes on a compact linear accelerator where the high- frequency power supply delivers the power to the linear accelerator through the external transmission line (external coupling) and at the same time serves as a source of electrons for it. The author concludes that such a device can function

properly in both configurations if it is realized as an oscillator as well as the amplifier driven by a high-frequency power source.

In parallel with Nygard, Richard Post filed his patent in February of 1955 [8]. His concept is pretty similar to the first one, considering one electron source for power collecting and accelerator sections aligned along the electron beam path (Fig. 1.4). The main difference of the new design is using the collector-coupler to transmit high-frequency power as well as a small portion of the initial electron beam. In comparison with the first design, Post's design has an internal coupling section rather than external transmitting line. In addition, the second author provides more details on how to realize such a coupler and discusses three different schemes comparing sizes and capabilities (Fig. 1.5).

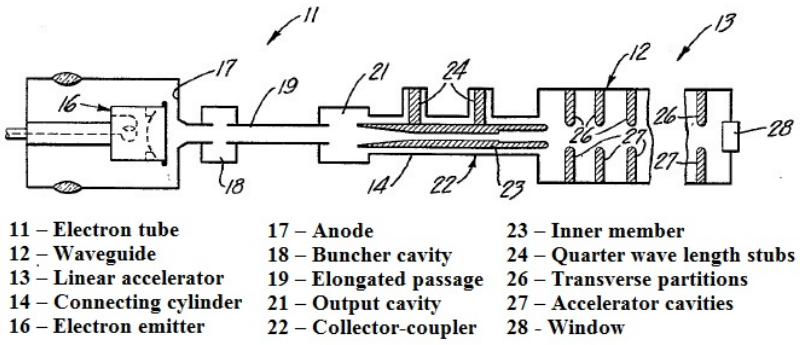

Figure 1.4: Post's electron accelerator scheme. Figure extracted from [8].

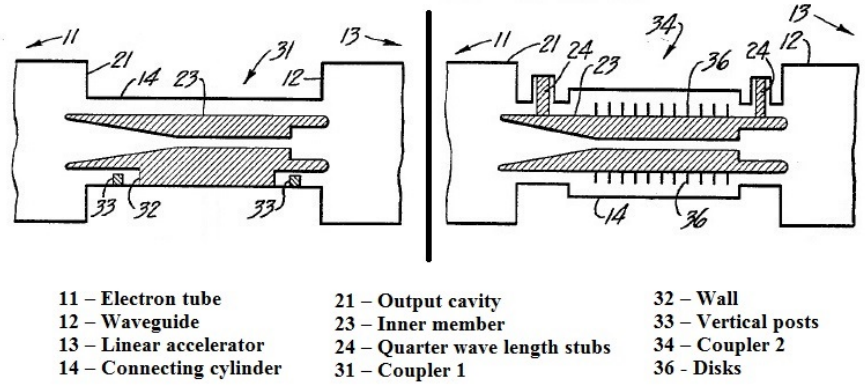

Figure 1.5: Post's schemes for coupler. Figure extracted from [8].

Richard Post claims that his advanced coupler will provide the correct phase shift between the voltage-doubled electron bunch transmitted through the collector and the high-frequency output signal from the klystron section. From the description of the design and the drawings it is not clear if his devise proposed to work as an oscillator or as an amplifier. The inventor only mentions that the initial beam is bunched the traditional way in the buncher cavity, which we assume, means implying the external driving source. However, it is not illustrated on the scheme. At the same time, there is no mentioning of any feedback inside the klystron part other than a possibility for an on-axis coupling, which means his device would require external high-frequency power source. Historically Nygard filed his patent a year earlier than Post and got it issued a half year earlier as well, which why we name John Nygard here as the first inventor and Post as the second. It is unknown to us if the authors were aware of each other's inventions, but both patents were issued by the United State Patent Office in the same calendar year of 1960. The main difference between the two concepts is the external and internal high-frequency power transmitting lines. Richard Post's design is more similar to our Klynac concept than Nygard's.

According to the US patent law for applications filed before June 8, 1995, and for patents that were still in force on June 8, 1995, the patent term is either 17 years from the issue date or 20 years from the filing date of the earliest U.S. or international application to which priority is claimed [9]. It is not clear to us exactly why neither the "compact linear accelerator" patented by John Nygard or the "electron accelerator" by Richard Post has ever been built. We assume it is the combination of several factors. The first reason is the complicated and unclear physical/technical realization for the transmission lines described by the inventors. The second factor, which is more likely, is the patent limited the possibility of building such a device for the remaining community. The next similar type of device, "A Klystron - Accelerator System", was described in a Canadian patent by Stanley Schriber in 1978 [10], which is a year after the first two patent rights had been discontinued. Interestingly, Schriber

does not provide any link to the previous patents by Nygard or Richard Post. Schriber proposes a device where the klystron section and accelerator section form a single structure, similar to the previous inventors' (Fig. 1.6). The high-frequency power transfer between the two parts is realized via coupling cells operating in $\pi/2$ mode, so there is negligible electric field and power loss in this coupling section. The inventor assumes creating an accelerator structure rather than an accelerator with a source of the electron beam. The electron gun serves only to drive the klystron section and does not serve as a simultaneous source for the accelerator as was proposed in the first patent by Nygard. It is assumed that an electron beam enters the accelerator section which is not aligned with a klystron beam line. The author does not limit his idea to the linear accelerator structure only but finds it possible to realize for another type of the accelerator machine. We assume that by another type Schriber means a circular accelerator. However the author does not provide a description or design of how this device would be realized in the last case and in particular how the klystron beam line(s) will be designed in the circular case. Summarizing the above, this invention is closer to the typical accelerator structure driving by the klystrons rather than to the Klynac type of device by requiring separate electron sources rather than one described in the first patent. On the other side, Schriber's coupling idea is better described and realized via using the coupling cells rather than Nygard's idea by using some undefined "transmission line" concept. To the best of our knowledge a device based on Schriber's idea has never been built either.

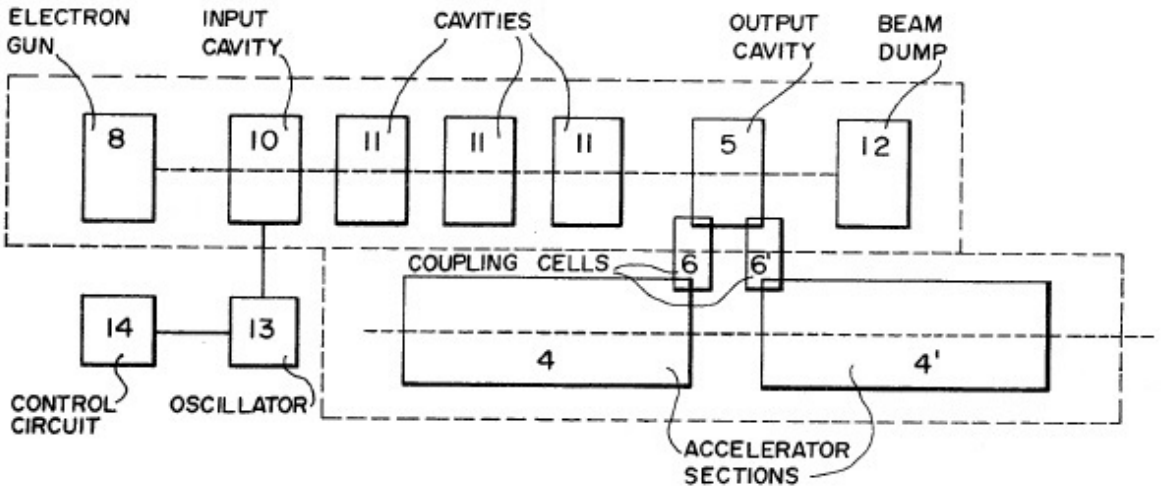

Figure 1.6: Schriber's klystron-accelerator concept. Figure extracted from [10].

1.3 A combined source of electron bunches and microwave power

More than 20 years after Schriber's patent was issued and almost 50 years after Nygard's and Post's patents had been submitted, Xie and his colleagues experimentally demonstrated a high- frequency klystron-based RF source producing electron bunches for acceleration [11]. In this device, small portion of the electron beam from the klystron section is transferred through a small hole in the collector followed by the bending magnet to the potential linac section substituted by the RF cavity for measuring a micro-pulse current followed by a Faraday cage to measure a macro-pulse current (Fig. 1.7). First, the authors operate the klystron as an amplifier; at the same time the possibility to operate it as an oscillator is discussed. For self-excitation, a small part of the microwave output power is fed back to the input cavity through a feedback circuit consisting of an attenuator, a phase shifter, and a resonant cavity providing the frequency stability of the system. Xie et al. used a particle-in-cell (PIC) code for the simulation of the electron beam motion in the 5 MW klystron under the typical operation condition of 126 kV and 89 A. They observed the presence of

the electron bunch at 70 keV driving the klystron as well as an electron bunch at higher energy $\sim$ 200 keV which can be used for further acceleration. The uniqueness of their scheme is using a bending magnet to select the beam with an appropriate (high) energy. Since the phase of such a beam is correlated with its energy, the selection device works as a phase filter as well as an energy selector at the same time. Xie and co-authors make the conclusion that an extremely compact linear accelerator can be constructed based on the designed and demonstrated dual-purpose klystron providing high-frequency power as well as an electron beam.

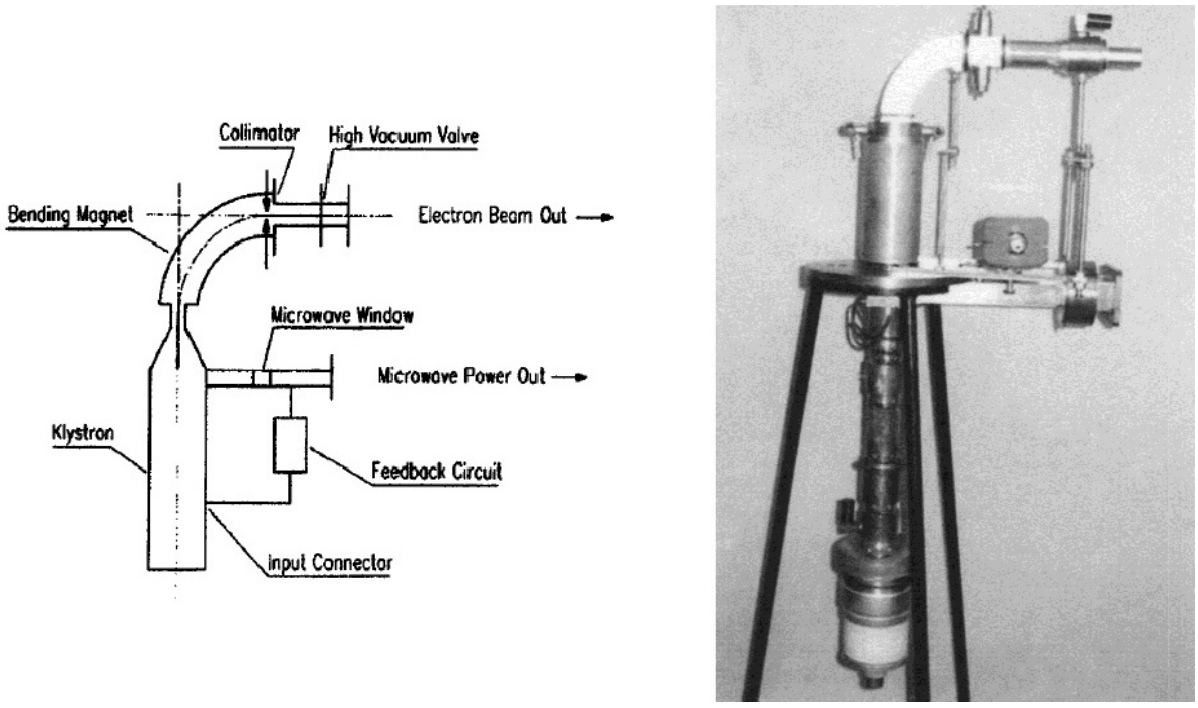

Figure 1.7: Xie's dual-purpose klystron: scheme and photo. Figure extracted from [11].

1.4 Summary

Summarizing the above, the idea of a compact linear accelerator, as a combination of a klystron and a linac, appeared more than a half century ago, right after the first linear accelerator driven by klystrons had been built. Since that time, scientists and engineers have proposed several possible design configurations, but the actual prototype has never been built. We were able to find three patents issued on a Klynac-like devise and are not completely sure that they are the only ones. The only prototype of a dual-purpose klystron, "the heart" of a Klynac-like device, has been built and demonstrated recently by Xie and his colleagues. Analyzing the previous concepts, we figured out that the main uncertainty of such a scheme is the realization of a transmission line providing high-frequency power from the electron beam at the klystron part to the linac part. Finally, it is not clear if a Klynac-like device can operate decently as an oscillator or can only work as an amplifier. At the very end, the main benefits of such a scheme are its size, cost and potential stability without additional external feedback systems.

CHAPTER 2

THEORETICAL MODEL AND DESIGN

In this chapter, we first will discuss the idea of a coupler. The coupler is responsible for transmitting the high-frequency power from the klystron part to the linac part, as well as a small fraction of the electron beam. Thus, it is one of the most important parts of the scheme to realize a Klynac-like device. Second, we discuss the power balance equation for our device to understand if it can work as an oscillator or requires some input driving power to build up. In addition, we discuss whether all the cavities in the device could be coupled to each other or the device should be realized as a multi-resonance structure. Finally, we use the coupled oscillators model to study competing modes in our device and how we can design it such a way that only one appropriate mode will build up.

2.1 Klynac resonant coupler

In our opinion, one of the main reasons why the compact accelerator concept proposed more than fifty years ago as a combination of a klystron and linac has not been realized is the lack of a proper coupler section. A coupler section, or as it was named previously the transmitting line, should extract all the power from the output cavity of the klystron and, in the best case scenario, transfer it with no loss to the resonantly coupled cavities of the linac section. At the same time, it should transmit a small fraction of the electron beam to the accelerator section and block the remaining part of the beam. In addition, it would be exciting to have an opportunity to control the fraction of the beam which goes through.

Finally, the coupler section should match the electron bunch arrival time with a phase of the electromagnetic field so the beam would be accelerated effectively. The last fact defines the size of a coupler section assuming some given speed of the electron bunch at the end of the klystron output cavity.

According to Potter et al., the key to the Klynac concept is that the klystron output cavity is resonantly coupled to the input cavity of the accelerator [12]. This means locking RF fields in the two sections in phase and defining the ratio between amplitudes. Now we will briefly discuss Potter's idea and how it can be realized. The concept of resonant coupling was invented at Los Alamos National Laboratory in 1967 for the Los Alamos Meson Physic Facility (LAMPF) [13]. The conventional on-axis resonantly coupled structure (Fig. 2.1) can be represented using a coupled circuit model on Fig. 2.2 [14].

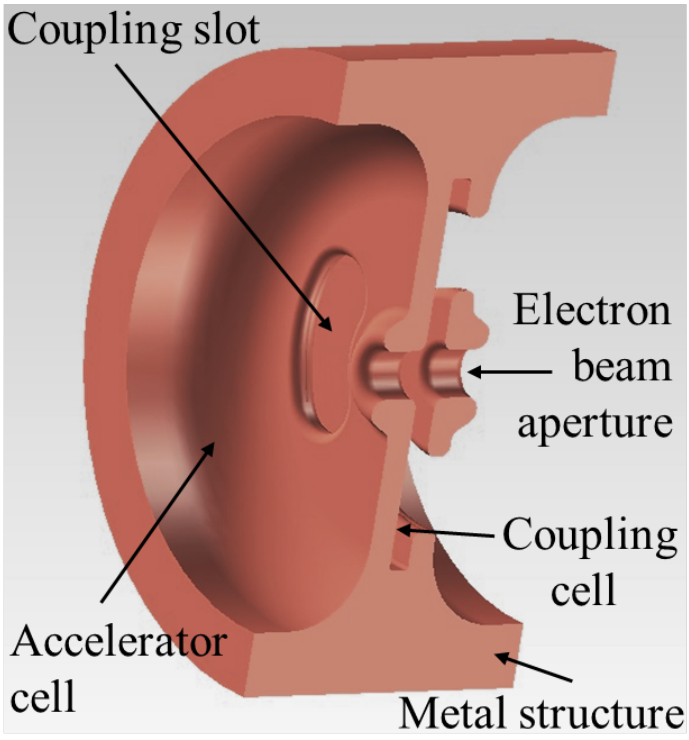

Figure 2.1: On-axis coupled accelerator structure. Figure extracted from [12].

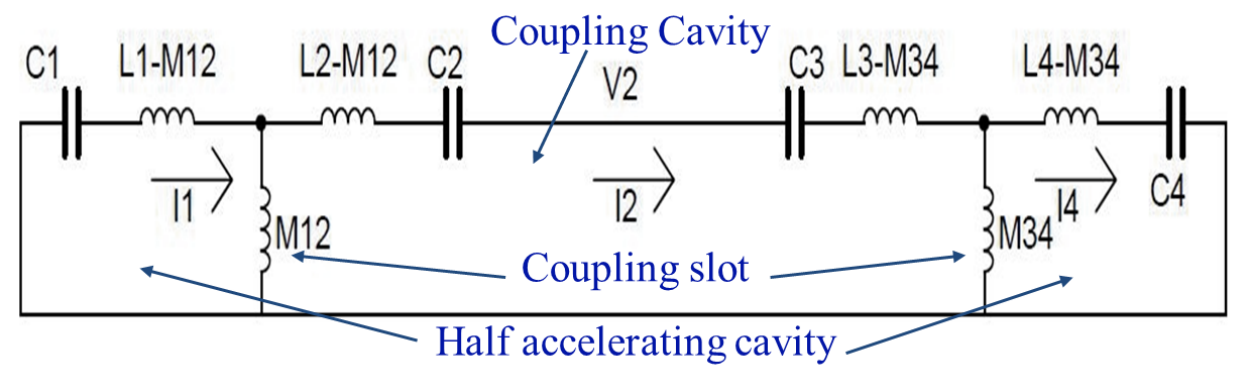

Figure 2.2: Coupled circuit model. Figure extracted from [12].

The Klynac coupler requires some drift space insert for the electron beam to arrive at the accelerator section at the correct time to experience an accelerating field. At the same time, it has to have a beam aperture to allow only a small part of the electron beam to go through. To fit the described requirements, the original coupler has to be modified. James Potter introduced an arbitrary insert, represented by an ABCD matrix, reproducing the transmission line, in the on-axis coupled cavity model described by the chain matrix (Fig. 2.3). He derives how the circuit parameters should connect to each other to observe the appropriate power transmission from the klystron output cavity to the input accelerator cavity in the case of perfectly tuned cavities. In addition, he discusses the behavior of the system if cavities on different sides of the coupler are not perfectly matched, making the device to oscillate on the weighted average frequency. Afterwards, Potter used high-frequency structural simulator (HFSS) [15], electromagnetic field calculator software, to simulate the 3D structure's electromagnetic field map to obtain the appropriate geometry for the coupler section of a Klynac-like device (Fig. 2.4).

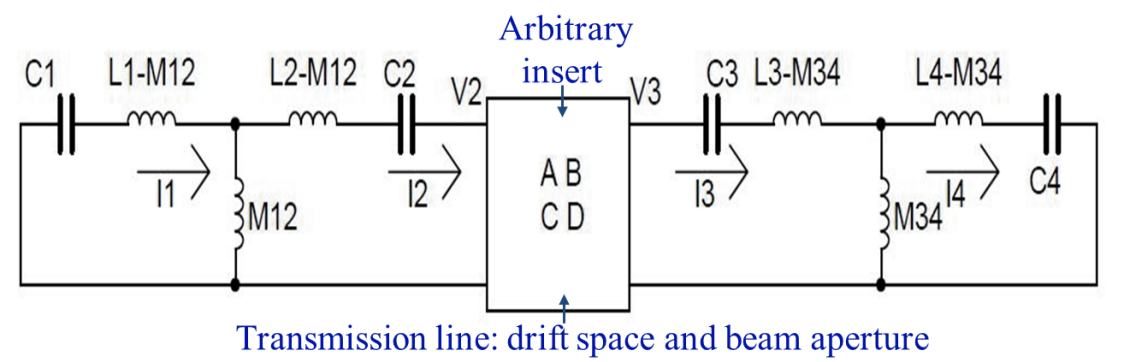

Figure 2.3: Coupled circuit model with transmission line added. Figure extracted from [12].

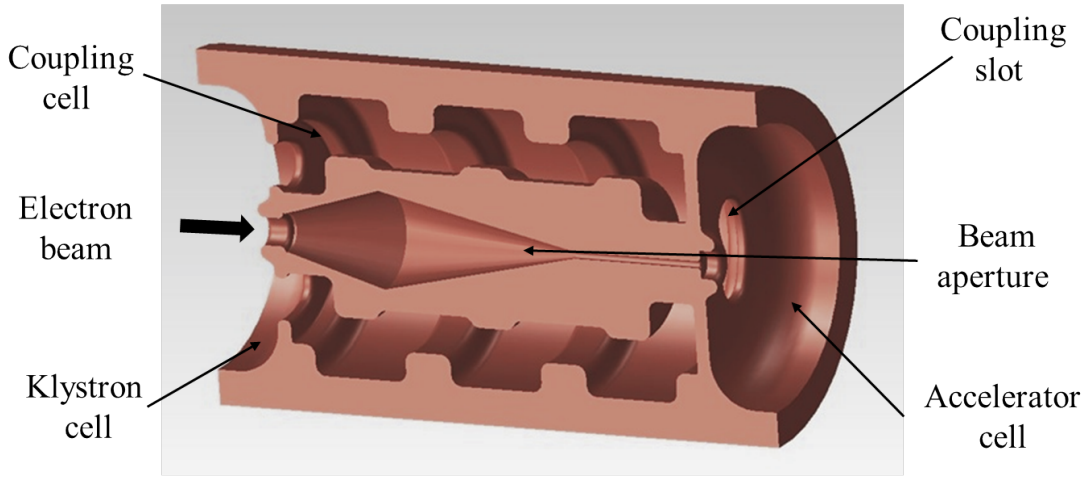

Figure 2.4: Coupler section for a Klynac-like device proposed by Potter. "The coupler is a TEM (coaxial) cavity tuned to transmit RF power and resonantly couple the klystron output cavity to the accelerator input cavity". Figure extracted from [12].

We have to admit that Potter's model works in the approximation that beam does not impact the electromagnetic field propagation through the coupler section. In other words, the section is not loaded by the electron beam, and in general there is no exchange in energy between the beam and the propagating electromagnetic field. In the next section we will show that the influence of beam loading on the accelerator section can critically impact on the power balance of the system and specifically on the propagation of the electromagnetic field as well as on the electron beam dynamics.

2.2 Power balance

In the previous section, we discussed how a klystron part and an accelerator part can be combined into the single device, Klynac, using a coupler section. A charged particles interaction with a field is the main feature to understand how a typical klystron works (Fig. 2.5). It consists of the three stages. First, some particles accelerate, some decelerate by the input field in the first cavity (called a buncher cavity), which causes a velocity modulation of the electron beam. Second, the electron beam with imposed velocity modulation propagates through the drift section, which results in a density modulation. Thus, initial DC current (electron beam) becomes bunched with input RF power period. Finally, on the third stage, RF power from the bunched beam is transferred back to the field in the output cavity (called a catcher cavity). Additional cavities (called idler cavities) in between buncher and catcher cavities are often inserted to increase the efficiency of the device by increasing the harmonic current in the bunched beam. While in the typical accelerator structure cavities are coupled to each other, in the standard klystron, in opposite, all cavities are uncoupled. Thus, only the first cavity is driven by the input RF field while all other cavities are driven by the electron beam.

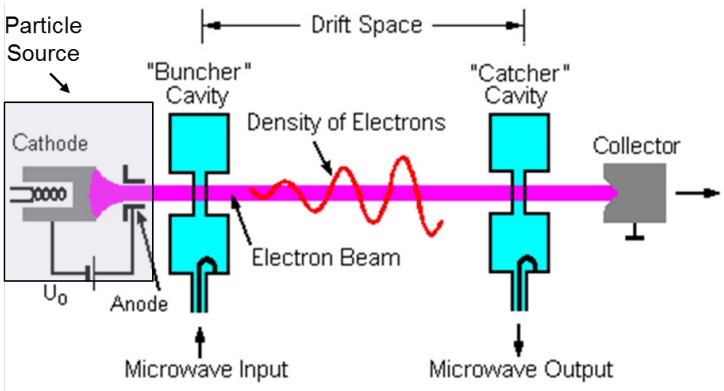

Figure 2.5: Klystron scheme.

Initially, James Potter planned on having a standard klystron structure configuration where the klystron cavities are not coupled to each other and only the output cavity of the klystron section is coupled to the accelerator section (Fig. 2.6) [12]. However, Bruce Carlsten proposed the idea of coupling cavities in the klystron section similarly to how it is realized in the linac section. The motivation for this was very exciting and promising. If the Klynac is realized as a single-resonance structure it has a potential to be less sensitive to temperature instabilities. Hence, no temperature control or feedback system would be required to tune the frequencies of the various parts. This coupled structure would be operated in the standard $\pi/2$ mode, where the fields in consequent klystron (accelerator) cavities are opposite in phase and have non-zero amplitudes, while the fields in the coupling cavities between them are negligible and do not impact beam dynamics. In other words, coupling sections are simply the drift sections for the electron beam. The only limitation on the klystron parameters is that the fields in consecutive klystron cavities are 180 degrees out of phase to each other. However, it should not be a serious limitation since the amplitudes can still be adjusted to maximize the extraction power in the output klystron cavity. In fact, maximizing the klystron efficiency in the simulation studies with the phases locked in all of the cavities was hard, but possible. The efficiency of such a klystron was lower than in the case where the output cavity had the freedom of phase choice of the field, but still close to 30%.

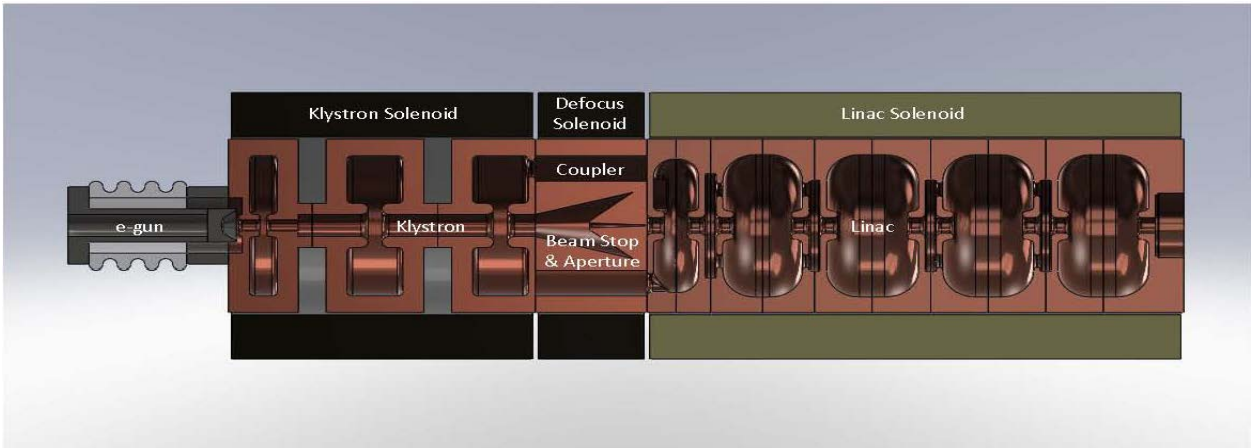

Figure 2.6: Klynac outline by Potter. Klystron cavities are not coupled to each other, but the output klystron cavity is coupled to the accelerator structure. Figure extracted from [12].

The initial motivation was to make the Klynac as simple as possible. Thus, we planned to operate it as an oscillator where the signal is built from noise as an instability. Klystrons have been operated in the oscillator regime for quite a long time, by redirecting a small fraction of the output power back to the input section [16]. Our configuration would not require any additional feedback; some output power would be automatically redirected through the coupling slots. As we will show in the next section, the amplitudes in different cavities of the coupled klystron are proportional to each other, which means, starting from a very small noise signal and interacting with an electron beam, RF field will increase proportionally to the coupling coefficients in every cavity, finally building up to a solid output signal. However, in addition to the klystron section we have an accelerator section loaded by some fraction of the beam going through the coupler section. We will analyze if such a configuration will turn on without any input power or, in other words, build up from noise using a power balance equation:

$$\frac{dU}{dt} = P_+ - P_- \ , \tag{2.1}$$

where U is the stored energy in the structure and $P_{+/-}$ are the power gained/lost over the RF period. The only source of power gain in our oscillator is the electron beam $P_+ = \eta I_k T_k V_k$, where η is the efficiency of the power transfer, V_k and I_k are klystron buncher cavity gap voltage and current respectively, and $T_k = \int_{-\infty}^{\infty} E_z(r,z)e^{i\beta_e z}dz / \int_{-\infty}^{\infty} E_z(r,z)dz$ - klystron cavity transit time factor. The transit time factor is a coefficient, taking into account that the electric field in the cavity changes in time as a particle (electron, traveling with a speed $\beta_e c$) crosses the cavity. At the same time, power losses are separated between klystron and accelerator sections $P_- = P_k + P_a$, and $P_a = P_c + P_b$, where P_k and P_c are power dissipated in the cavities in the klystron and accelerator sections, respectively, and P_b is the power required to drive the electron beam in the linac section. Thus, assuming the negligible power loss in the klystron cavities, as well as in all the coupling cavities, the power equation becomes:

$$\frac{dU}{dt} = \eta I_k T_k V_k - (n+\epsilon)\frac{V_l^2}{Z_l} - (n+\epsilon) I_l T_l V_l \ , \tag{2.2}$$

where Z_l is the linac cavity impedance, n is the number of accelerating cavities with the same amplitude V_l, and ϵ is a relative amplitude in the input linac cavity tuned to catch the low energy non-relativistic electrons arriving from the klystron section.

Since all the cavities are coupled to each other, then $V_l = \alpha_c V_k$. At the same time, $I_l = \alpha_t I_0$, where α_c is the coupling coefficient, I_0 is the current from the electron gun entering the klystron input cavity, and α_t is a beam aperture transmission ratio in the coupler section between the klystron and linac sections. Therefore, for small voltages in the cavities, power loss is defined by the electron beam loading the accelerator section $P_- \sim V_k$. Power gain is proportional to V_k, as well as I_k, the current driving the klystron, which is proportional to $V_k I_0$, which can be shown from the no space charge ballistic bunching approximation [6]:

$$I_k = I_0 J_1\left(\frac{T_k \alpha_g V_k e w l}{m c^3 \gamma^3 \beta^3}\right) \ , \tag{2.3}$$

where T_k is the klystron cavity transit time; $\alpha_g V_k$ is the output klystron cavity gap voltage; and e, m, β, γ are electron charge, mass, relative speed and relative energy respectively. Thus, at lower amplitudes, power gain is proportional to V_k^2 and cannot match the power loss caused by the electron beam loading the accelerator part proportional to V_k, and the Klynac, in such a configuration, will never build up from noise.

The analysis showed that to maintain a proper power balance in the steady-state regime for all coupled cavity configuration, an input RF field device is required with a power around half of what the klystron section of a Klynac would produce. This fact makes all coupled cavity configuration not appropriate, unless one wants to work in the pulsed regime. If the field builds up from noise in the klystron and accelerator section before the actual electron beam reaches the accelerator section, then some part of the electron beam upon arrival will be accelerated until all the stored power in the system is used. Such a configuration would be a single-pulse accelerator and would require turning off the electron beam from the electron gun repeatedly. On the other hand, it is possible to control the transmission coefficient of the beam inside the aperture in the coupling section between the klystron and accelerator sections, which potentially can maintain the proper power balance and put the beam in the accelerator section, once enough power for the acceleration is stored. This configuration can potentially give a higher repetition rate than the previous one. However, our initial intent was to provide the universal compact accelerator concept, which would be able to work in the continuous regime. The last fact forced us to uncouple the last idler cavity of the klystron section from the output cavity, which is coupled to the accelerator section. Such a configuration would be less stable than the original one but would not require a lot of input power and, potentially, can even build up from noise.

Historically, the all-coupled cavity structure got the name “type-1”, while the second bi-resonance structure - “type 2”. Type-2 configuration has been designed and built, whereas the type-1 has been only studied numerically. In addition, Bruce Carlsten and Kimberley

Nichols recently came up with an alternative bi-resonant configuration where the buncher cavity of a klystron section is uncoupled from all remaining cavities, which are all coupled to each other [17]. We will discuss the simulation results for type-1 and type-2 configurations in the next chapter, but first we will finish this chapter with a last theoretical section discussing the theory of coupled oscillators, analyzing if our device is sensitive to other modes rather than the main $\pi/2$ mode for which we designed it. The theoretical analysis assumes negligible fields in the coupling cavities.

2.3 Coupled oscillators model and competing modes

We designed our device with four klystron cavities and four accelerator cavities. The first three klystron cavities are coupled and the remaining output cavity of the klystron is coupled to the four accelerator cavities satisfying the bi-resonant structure of the type-2 device, described above. For acceleration to an energy of more than 1 MeV one may add more accelerating cavities and increase the electron energy and/or current of the beam from e-gun entering the klystron section. Three klystron cavities was an optimum number to achieve desirable harmonic current in the output klystron cavity and realize the 30% efficiency klystron for the given electron beam parameters of 50kV and 100A. Since the first three cavities are connected via two coupling cells, we have a total number of five coupled cavities - five coupled oscillators. In such a system, in general, five eigen modes oscillating on five different eigen frequencies can exist and compete with each other to build up from noise and/or input signal extracting power from the electron beam. Only the $\pi/2$ mode has the feature that the field in the coupling cavities is negligible and there is no significant interaction of it with an electron beam traveling through. Before going into the analysis of

competing modes, we will briefly remind ourselves the theory of coupled oscillators based on the simplified mechanical oscillators model.

A simple mechanical oscillator example is a mass attached to the spring (Fig. 2.7). The equation of motion is described as differential equation of a second order:

$$\frac{d^2x}{dt^2} + w^2x = 0, \tag{2.4}$$

where $w = \sqrt{k/m}$ is the natural frequency of the system defined by the mass and spring constant. This equation of the second order can be represented as a system of two differential equations of the first order:

$$\begin{aligned} \tfrac{dp}{dt} + w^2x &= 0, \\ p - \tfrac{dx}{dt} &= 0. \end{aligned} \tag{2.5}$$

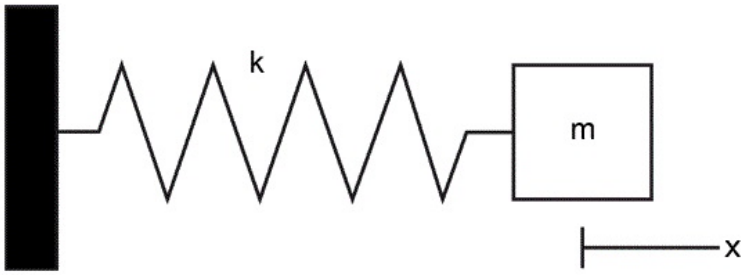

Figure 2.7: Mechanical oscillator.

The solution for the system of linear differential equations is searched in the $e^{-\lambda t}$, form and putting it in the equation, we obtain the problem of searching for eigen values and eigen vectors:

$$det(M - \lambda E) = 0, \tag{2.6}$$

where

$$M = \begin{pmatrix} 0 & w^2 \\ -1 & 0 \end{pmatrix}, \quad E = \begin{pmatrix} 1 & 0 \\ 0 & 1 \end{pmatrix},$$

which of course will give us well-known $\lambda^2 = -w^2$, which we would get right away by putting $e^{-i\lambda t}$ in the original equation of the second order. We find out that eigenvalues for such a system are $\lambda_1 = i\sqrt{w^2}$ and $\lambda_2 = -i\sqrt{w^2}$. Then we find eigen vector (p_1, x_1) by solving the linearly dependent $(det = 0)$ system of equations:

$$\begin{pmatrix} -\lambda_1 & w^2 \\ -1 & -\lambda_1 \end{pmatrix} \begin{pmatrix} p_1 \\ x_1 \end{pmatrix} = \begin{pmatrix} 0 \\ 0 \end{pmatrix} , \tag{2.7}$$

which simply obtains the linear coefficient connecting p_1 and x_1 from the first (second) equation of the system giving us the eigen vector related to λ_1 as $(-iwx_1, x_1)$. Then one may like to normalize this vector to unity or simply leave it as it is. Following the same procedure, the second eigen vector (iwx_1, x_1) related to λ_2 can be found. Then the final answer is a linear combination of two eigenvectors where coefficients are defined by initial conditions at t=0 via equation:

$$\alpha \begin{pmatrix} -iwx_1 \\ x_1 \end{pmatrix} + \beta \begin{pmatrix} +iwx_2 \\ x_2 \end{pmatrix} = \begin{pmatrix} p_0 \\ x_0 \end{pmatrix} , \tag{2.8}$$

or by simple inserting unidimensional coefficients α and β in the eigen vectors and redefining x_1 and x_2, leaving us with a system of two equations for two unknown variables:

$$\begin{pmatrix} -iwx_1 \\ x_1 \end{pmatrix} + \begin{pmatrix} +iwx_2 \\ x_2 \end{pmatrix} = \begin{pmatrix} p_0 \\ x_0 \end{pmatrix} . \tag{2.9}$$

Such a sophisticated analysis of a simple harmonic oscillator is useful once we start making the system more complicated. First, we add friction in the equation:

$$\frac{d^2x}{dt^2} + \gamma\frac{dx}{dt} + w^2x = 0, \tag{2.10}$$

where γ is the friction coefficient. Rewriting the previous second-order ordinary differential equation as two coupled first-order equations gives:

$$\begin{aligned} \tfrac{dp}{dt} + \gamma p + w^2 x = 0, \\ p - \tfrac{dx}{dt} = 0, \end{aligned} \tag{2.11}$$

which is still the eigen problem or the problem of how to diagonalize a matrix. The only thing that changed is the matrix:

$$M_{friction} = \begin{pmatrix} \gamma & w^2 \\ -1 & 0 \end{pmatrix}.$$

Moving forward we have n harmonic oscillators (Fig. 2.8), which are described as a system of $2n$ linear differential equations. If there is no coupling then it can be solved as n independent two-dimensional systems, and if it is coupled, then we still have an eigenvalue problem for the matrix M_{2n} which can be solved for any dimension n for a finite time. It is obvious right away for x- and p-coupling by looking at the equations:

$$\begin{aligned} \tfrac{dp_i}{dt} + \gamma_i p_i + w^2 x_i - \sum_{j=1, j\neq i}^{n} (\alpha_j x_j + \beta_j p_j) = 0, \\ p_i - \tfrac{dx_i}{dt} = 0, \end{aligned} \tag{2.12}$$

and even for the system with dp/dt coupling:

$$\begin{aligned} \tfrac{dp_i}{dt} + \sum_{j=1, j\neq i}^{n} c_j \tfrac{dp_j}{dt} + \gamma_i p_i + w^2 x_i - \sum_{j=1, j\neq i}^{n} (\alpha_j x_j + \beta_j p_j) = 0, \\ p_i - \tfrac{dx_i}{dt} = 0, \end{aligned} \tag{2.13}$$

it can be shown that it still remains the eigen problem using substitution:

$$p_i + \sum_{j=1, j\neq i}^{n} c_j p_j = p_i' \ . \tag{2.14}$$

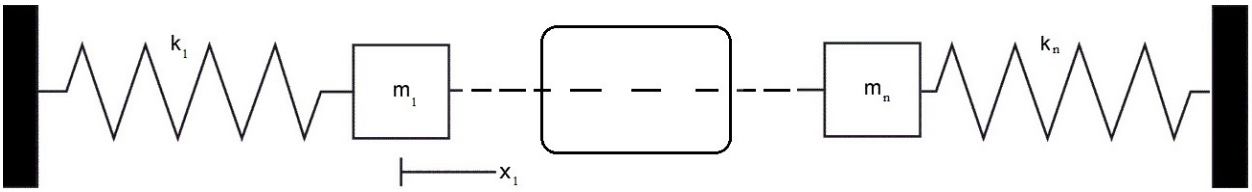

Figure 2.8: Mechanical coupled oscillators.

We have to admit that for a big n the matrix diagonalization algorithm could be used to solve equation $\sum_n \alpha_j x_j^j = 0$ rather than vice versa. But it is not always easy to find the matrix for the polynomial, which is why we would like to keep the description for our coupled oscillators as a system of first-order linear differential equations.

The single cavity can be represented as an electrical oscillator circuit (Fig. 2.9), which makes our coupled cavities a system of coupled oscillators. Above we discussed all the possible coupling situations, which means eigen values and eigen modes can be found even for a rather complicated system. For our competing mode analysis we have to understand several basic principles. First, our main mode has to have frequency distinct from all other modes which we call parasitic modes or competing modes; in addition it should not be close to $n \cdot w$, where n is an arbitrary integer number. Second, the scale for the significant frequency difference is defined by the Q factor of the coupled cavity system. In addition, the driving device should provide power at the desired frequency with initial conditions stimulating oscillations only for the desired mode. Finally, if competing modes grow slower than the main mode from the input oscillations or noise then we do not have to worry a lot about it taking some power from our main $\pi/2$ mode.

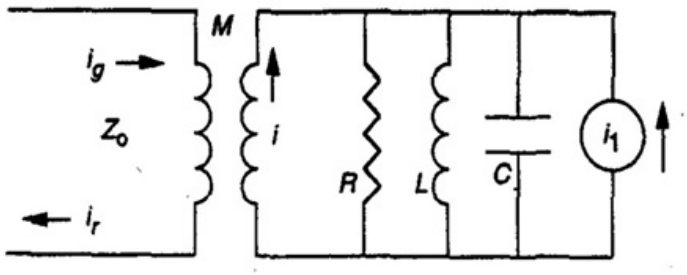

Figure 2.9: Electrical oscillator circuit for single cavity with coupling.

The main difference between this mode and competing modes is a zero field in the coupling cavities. To prevent parasite modes from growing, one may like to reduce the transit time factor for coupling cells for this mode. Bruce Carlsten proposed to minimize it by coupling cavity geometry adjustment, specifically by varying the separation of the coupling cell's nose cones. If we assume that the electric field between noses is [18]:

$$E(z) = \frac{2V_{gap}}{\pi d}(1 - \frac{2z^2}{d})^{-1/2} , \tag{2.15}$$

then the transit time factor depends on the gap, d, as:

$$T \sim J_0(\frac{wd}{2c\beta}) , \tag{2.16}$$

and can be minimized by choosing the gap around 2 cm at roughly 3 GHz frequency. At the end of the next chapter we will discuss the simulation studies for competing modes in the klystron part and show that it does not critically impact the Klynac performance for our geometry configuration.

Summarizing the theoretical part, based on James Potter's idea for the coupler between the klystron and accelerator sections, we proposed the configuration of a Klynac as a single-resonant structure where all the cavities are coupled to each other and as a bi-resonant

structure with the first three cavities of the klystron section being coupled and the output klystron cavity coupled to the accelerator cells. We demonstrated that the first configuration will never turn on by analyzing the power balance equation. We demonstrated that for any coupled oscillators system the eigen modes and eigen values could be found during the diagonalization of a matrix defined by the oscillators' and coupling parameters and can be solved for an arbitrary amount of oscillators. Using the model of coupled oscillators we described some mechanisms to prevent appearance of the competing modes in the Klynac device, and in addition, we discussed a theoretical approach to minimize their influence by choosing the coupling cell geometry to minimize the transit time factor for competing modes.

CHAPTER 3

SIMULATION STUDIES

In this chapter, we will discuss the simulation studies of a Klynac-like device. After understanding some basic ideas about how the Klynac device could be realized, the major part of the design was done using simulation tools. We will start this chapter with a brief description of the codes and software used, then we will describe the simulation process step by step following the original path for the Klynac design. First, we had to find voltages ratio in the cavities and simple geometry parameters, such as cavity and gap sizes, distances between cells, etc., to reach the desirable behavior of our Klynac device. The second step was to realize these parameters in a real 3D geometry structure with appropriate coupling coefficients to reach the desirable voltages and power distribution in the system. In this thesis we will concentrate on the first step only, since the majority of the second-step work was done by other colleagues. At the end of this chapter, we will show that simulations can be used not only for the design purposes but also as a powerful tool to understand the physics of the system and, in particular, the behavior of competing modes.

3.1 Simulation tools

In this section we will provide a short overview of simulation tools we used to design the Klynac-like device and mention others that can potentially be used. First of all, our Klynac device is connected to the electron gun. For some particular device it might be necessary to simulate the beam dynamics of the electron gun or another source of the electron beam to get

the correct beam distribution at the input of the Klynac. For these purposes, for instance, EGUN developed at Stanford Linear Accelerator Center (SLAC) can be used [19], or OPAL, developed as an international collaboration [20] , can be used in case of a photo-cathode. In our design we assumed Gaussian model for the electron beam entering the klystron input cavity.

Moving forward, the first part of the Klynac-like device is a klystron. AJDISK, developed by A. Jensen at SLAC, is one of the most popular simulation tools used to design a klystron [21]. The input and output for the program is presented in Fig. 3.1 on the left and right respectively. Following the description of the program from [6], the code is transporting the beam through the klystron using a 1D charged disk model. The motion of each disk is governed by the space charge fields from the other disks and cavity electric fields. Cavity field is determined by the gap voltage and longitudinal Gaussian profile model. The Gaussian parameter k can be found using Superfish [22] for the given cavity geometry (we will discuss Superfish code later in this section). Initially cavity voltages are set close to zero, except the input cavity where it is calculated from the input power specified by the user, then fields are calculated for each cavity. After that, using the equation of motion with a Lorentz force applied, beam motion is calculated. At the next step, based on the motion of the beam, the induced current and then its fundamental harmonic are calculated. Cavity voltages are then calculated using the cavity impedances defined from the input parameters and induced current from the previous step. The new cavity voltages are compared with the initial ones, and if there is a significant difference, the procedure is repeated with new cavity voltages. Once calculated voltages match with input voltages, stability is reached. On the final step the gain and efficiency are calculated.

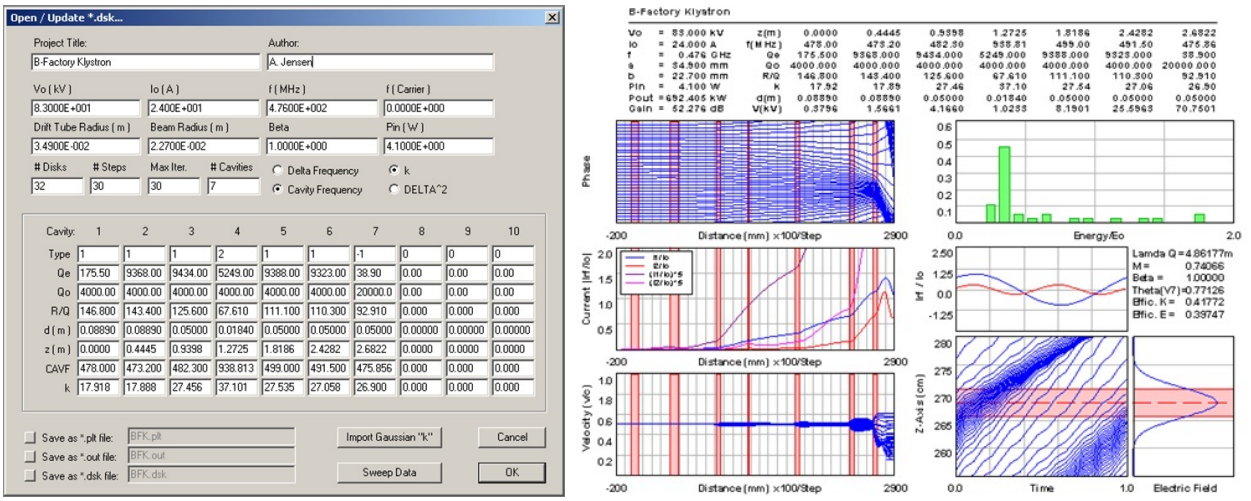

Figure 3.1: AJDISK input (on the left) and output (on the right) for a B-Factory klystron. Figure extracted from [21].

We used AJDISK in the beginning of our studies to find the input parameters for the cavities and its optimum locations to reach voltages in the cavities with π phase difference to the nearest neighbors to satisfy $\pi/2$ mode principles . Of course, we assumed all the coupling cavities as drift sections only. This method was not successful and very time-consuming, mostly because AJDISK is not designed for these purposes, to reach some phase synchronism. In general, it is possible to realize an external algorithm search for AJDISK to find the appropriate phase ratio in the cavities but instead we decided to use a particle-in-cell (PIC) simulation code specially developed for our design purposes, named Klynac.

The Klynac code was Bruce Carlsten's modification of a PIC code used at LANL for designing klystrons and understanding the associated beam dynamics, as in typical PIC-codes, by pushing particles via the Lorentz force equation. The fields are calculated on a grid, usually separately for the space charge and RF fields. Space charge fields are calculated using a Green's function approach. The algorithm for searching for self-consistent cavity gap voltages is similar to what we discussed above for AJDISK; the main difference is that now the dynamics are in 2D (r, z) and we are pushing particles through the cell to find the

induced current, which updates our fields. Starting with a zero magnetic and electric field in the cell, we calculate the new fields from a beam current using the Maxwell equations:

$$\begin{aligned} \frac{\partial \vec{B}}{\partial t} &= -\vec{\nabla} \times \vec{E}, \\ \frac{\partial \vec{E}}{\partial t} &= c^2(\vec{\nabla} \times \vec{B} - \mu_0 \vec{J}), \end{aligned} \tag{3.1}$$

where J is an induced current in the cell, and in general multiple drive frequencies can be taken into account. Current is defined inside the cell while the density charge is determined on the borders.These parameters have to satisfy the continuity equation:

$$\frac{\partial \rho}{\partial t} + \vec{\nabla} \cdot \vec{J} = 0. \tag{3.2}$$

For our particular design needs, we would have to be able to push the particles through the cells with given cavity gap voltage, amplitude, and phase at given locations and be able to calculate the induced current in each cavity and gain. Thus, the PIC code was modified to satisfy this concept. To make sure the appropriate cavities can be designed to fit in the Klynac outline, we use Poisson Superfish code.

Superfish is a software developed at Los Alamos National Laboratory. It solves a set of inhomogeneous field equations by the direct, noniterative method to solve the difference equations in an irregular triangular mesh with given Dirichlet or Neumann boundary conditions for a given cavity geometry [22]. Once we have the specific cavity geometry and define the boundary conditions, we can get a field map on the grid. Then we can directly upload the field map to the Klynac code for each cavity and normalize it using cavity gap voltage parameters. After that, we can push particles through the cells using the exact field map.

3.2 Designing klystron part

Following the description of the simulation tools in the last section we jump to the Klynac design description starting from the klystron section. We will concentrate on a description of using the PIC-code KLYNAC to design our prototype. The purpose of the simulations here is to set up locked phases in the klystron cavities with a π phase relative shift. After that by choosing the appropriate cavity positions and voltage amplitudes the goal was to maximize the induced current in the output cavity. In the first step, we only had in mind the all-coupled cavity design. Thus, we did simulations for the klystron part where all cavities are coupled to each other. After a significant part of studies was completed, we were about to realize that design as a real 3D structure and start building. Then we understood that it will never turn on by analyzing the power balance equation. The electron beam loading the acceleration section requires significant input power in the klystron section to maintain positive power balance, as it is fully described in Chapter 2, Section 2.2. Despite the last fact, we still would like to describe all the processes for the type-1 structure simulation study, since a lot of interesting physics came up during the study. The understanding gained from the type-1 structure work made designing type-2 structure smooth and fast.

Before describing the type-1 structure design process, we want to mention how the Klynac is driven. As mentioned before we hoped to build up the oscillations from noise without any input power. In this approximation, the first cavity had to have very low voltage, which in our simulations was around 100 V. Next, the cavities were driven by the beam and were able to have significant voltages. The second approximation of the Klynac as an amplifier assumed presence of some input power and another design outline, in particular, might be required. Actually, the modification of an oscillator design to the amplifier one is simply

removing the first cavity with a low voltage. That is why in the initial oscillator scheme we had five cavities and ended up with four in the second case.

3.2.1 All-coupled cavity design

In the case of the type-1 structure the output klystron cavity was locked in phase and it was quite hard to reach high-efficiency of the klystron section with this restriction. At the very beginning we were trying to get high klystron efficiency results as soon as possible, so we used different gap sizes for different cavities and some of them were not realistic parameters. In addition, we did not care too much about the voltage in the input cavity being a particular small value or for any other parameters to be specific as well. In opposite, we wanted to first check if it was even possible to get the klystron to work with locked cavity phases in our simulations.

The typical optimization to maximize induced current had a pretty simple outline. The cavity location is defined by the position of its center. We started with a cavity located at some distance from the electron gun to leave some space for the potential adding of a magnet and/or to fit the real cavity geometry, since the gap size is typically smaller than the real cavity size. We put some initial voltage in the first cavity: small in the case when we were designing the device as an oscillator and significant if it was designed with some input power. To the first cavity we added the next cavity and adjusted its position and voltage amplitude to maximize the induced current in it. Then we moved to the next cavity repeating the procedure. Once the induced current in it was maximized by these cavity parameter adjustments, we perturbed previous cavity parameters to reach a better induced current. This procedure was repeated several times after adding each cavity.

Our first design, after some optimization (input file presented in Fig. 3.2), had an efficiency of 46% (output file presented in Fig.3.3). Of course, the output cavity gap size of 3 mm was extremely unrealistic. After that we made a decision that all gap sizes should be the same, which would significantly simplify designing and building the actual prototype. We estimated that a cavity with a gap size of 18 mm maintains a realistic build configuration. The cavity gap size was fixed in the range of 18-22 mm and it had to be the same for every cavity. Once we made all the gap sizes 19 mm we immediately observed an efficiency drop to 18% (Fig. 3.4).

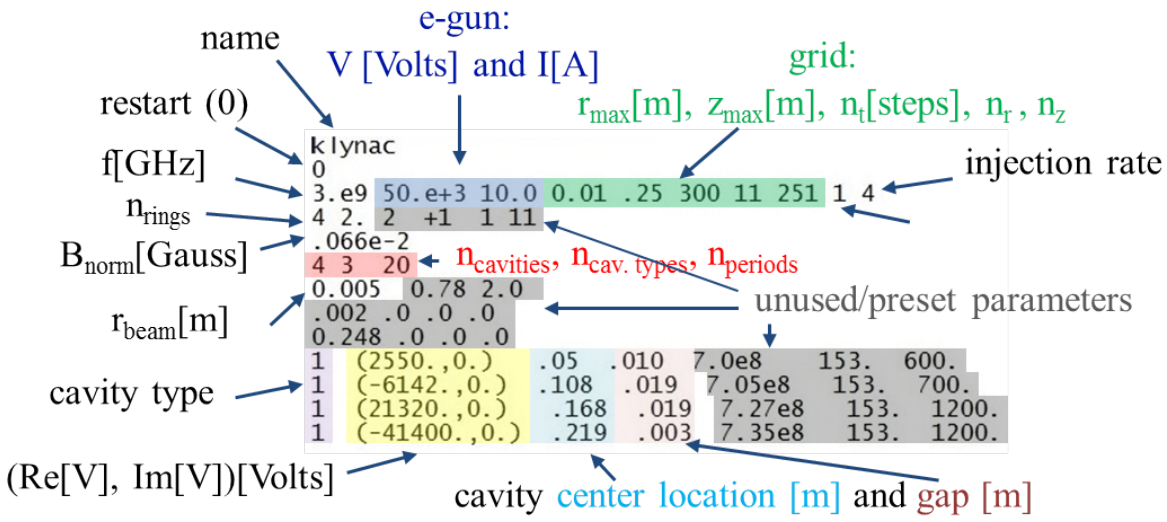

Figure 3.2: KLYNAC input file with a legend for the first high-efficiency design.

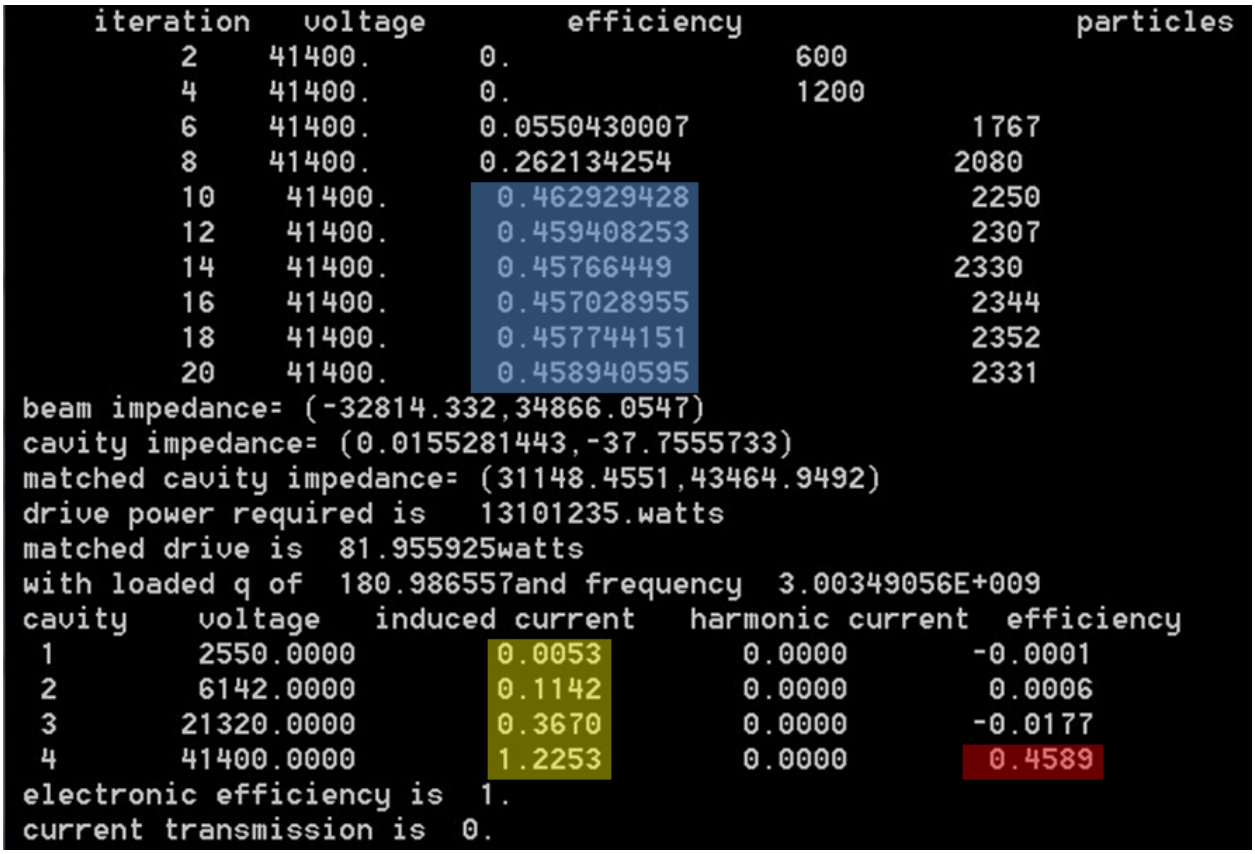

Figure 3.3: KLYNAC output file for the first high-efficiency design. Several iteration results are shown to make sure that simulations reached stability (highlighted blue). Harmonic current (highlighted blue) and efficiency (highlighted red) are parameters to be maximized.

For the future Klynac-like devices, this limitation can be removed and free parameters can be used to increase the efficiency or to help satisfy any other particular design needs. The idea of decreasing the cavity gap while maintaining the same voltage means increasing the field. In the case of infinitely small gap, one would have to have infinite electric fields. The RF field energy exchange with a beam will be a kick-type interaction in space and time. Of course, at extremely big fields the ohmic losses would become significant, so an optimum gap size not equal to zero would exist.

```
         18    44400.      0.18648842                1983
         20    44400.      0.186636403                1983
beam impedance= (-28675.5781,917.751343)
cavity impedance= (5209.06152,26001.7109)
matched cavity impedance= (132009.141,19870.0762)
drive power required is   164.460571watts
matched drive is  137.347763watts
with loaded q of  111.889847and frequency  3.00030106E+009
cavity    voltage   induced current   harmonic current  efficiency
 1        2550.0000        0.0089        0.0000       -0.0002
 2        6142.0000        0.0883        0.0000       -0.0005
 3       21320.0000        0.3220        0.0000       -0.0085
 4       44400.0000        0.4997        0.0000        0.1866
electronic efficiency is  1.
current transmission is  0.
```

Figure 3.4: KLYNAC output file for the first design with similar gap size.

Once we fixed the gap sizes to the certain number, we had to redo the design to optimize its efficiency from 18% to at least 30%. We still had cavity locations and voltage amplitudes as free parameters to play with. After some effort and time, we obtained a really good , at least on the first look, configuration (Fig. 3.5) delivering the efficiency of 49% in the output cavity (Fig. 3.6). However, we can see that the second and the third cavities have negative efficiency of 3% and 27% respectively, which means the total efficiency of the klystron part is still very low, around 19%. Positive efficiency in our code means that an electron beam is working on the field, whereas negative efficiency means opposite: electric field is working on the electron beam. Since we are not driving these two cavities directly they have to drain power from the neighbors, input and output cavities.

Optimizing this device one would have to remember that the overall efficiency of all the cavities in the Klynac part matters not only for the output cavity. In the regular klystron, where cavities are not coupled to each other, negative efficiency in the idler cavities is not appropriate, since there is no input power. Hence, field and harmonic current should be $\pi/2$ out of phase, so the total average power exchange between the beam and RF field is equal to 0. In the input cavity, driven by RF source or by a part of the field from the output cavity in case of an oscillator, efficiency should be a small negative number, meaning electric field power transfers to the beam. Finally, in the output cavity, efficiency should be a positive

```
klynac
0
3.e9 50.e+3 10.0 0.01 .25 300 11 251 1 4
4 2. 2  +1  1 11
.066e-2
4 3  20
0.005  0.78 2.0
.002 .0 .0 .0
0.248 .0 .0 .0

1  (8088.,0.)    .050  .019  7.0e8    153.  600.
1  (-10059.,0.)  .116  .019  7.05e8   153.  700.
1  (40256.,0.)   .180  .019  7.27e8   153.  1200.
1  (-55328.,0.)  .227  .019  7.35e8   153.  1200.
```

Figure 3.5: KLYNAC input file for the high-efficiency in the output cavity configuration.

```
         18    55328.      0.493921548                1852
         20    55328.      0.494304478                1852
beam impedance= (-27958.1387,1888.87952)
cavity impedance= (0.0155281443,-37.7555733)
matched cavity impedance= (87530.4766,19331.6719)
drive power required is   131672968.watts
matched drive is  1520.86658watts
with loaded q of  113.883224and frequency  3.00055219E+009
cavity    voltage   induced current   harmonic current  efficiency
 1        8088.0000        0.0289        0.0000       -0.0023
 2       10059.0000        0.3281        0.0000       -0.0286
 3       40256.0000        0.7413        0.0000       -0.2707
 4       55328.0000        0.9206        0.0000        0.4943
```

Figure 3.6: KLYNAC output file for the high-efficiency in the output cavity configuration.

quantity ideally around 50% because if a much larger number is observed the beam will turn around in the last section [6]. In our klystron structure, where all the cavities are coupled, different rules are applied. The only limitation is the significant positive overall efficiency and the condition that such a voltage amplitude ratio between cells can be realized for realistic coupling and cavity structure parameters.

We thought that an"exact synchronism" of the electron beam with RF electric field in time and space can help us to increase the efficiency of our Klynac prototype. We tried to combine the configuration where all the cavities are separated on the same "magical"

distance of 5.25 cm from their neighbors (Fig. 3.7). Actually, there is no magic but physics in this number. For RF frequency we are planing to have in our device, $f = 2.856$ GHz, we obtain the wavelength:

$$\lambda = \frac{c}{f} = \frac{3 \cdot 10^{10} cm/sec}{2.856 \cdot 10^{9} sec^{-1}} = 10.5\ cm, \tag{3.3}$$

which means if we have the distance of 5.25 cm and the phase shift of π (remember we have a virtual coupling cavity instead of the drift section) between two klystron cavities we will maintain the phase synchronism for our $\pi/2$ mode structure, of course, if the electron beam is moving with the speed of light. We will use this exact distance once the beam is moving with the speed of light in the accelerator section further to maintain proper synchronism. Initially the speed of the beam is less than the speed of light, $\beta \sim 0.42$, leaving an electron gun with applied voltage of 50 kV. For other voltages different speed will be observed. The speed of the beam is changed during its propagation through the klystron section. Since it stays about half of the speed of light, then synchronism is not observed. Controversially, once the beam is reaching the second cavity located at 5.25 cm, the phase of the field in it will change on 2π instead of π for the speed of light beam, and the field will be the same as it was at t=0. The last fact means that voltage phases defined at t=0 in the lab frame are close to the voltage phases the beam sees entering each section. We got pretty good results of 25% overall efficiency with some small negative and positive numbers from the second and third cavities respectively and the decent positive one from the output cavity (Fig. 3.8).

```
klynac
0
2.856e9 50.e+3 10.0 0.01 .28 300 11 281 1 4
4 2. 2  +1  1 11
.066e-2
4 3  20
0.005  0.78 2.0
.002 .0 .0 .0
0.248 .0 .0 .011:18 04.09.2016

1  (288.,0.)   .0525  .019  7.0e8    153.  600.
1  (-8300.,0.)  .1050 .019  7.05e8   153.  700.
1  (21356.,0.)   .1575 .019  7.27e8   153.  1200.
1  (-50328.,0.)  .2100 .019  7.35e8   153.  1200.
```

Figure 3.7: KLYNAC input file for cavity separations equal to a half wavelength of the propagating mode $f = 2.856$ GHz.

```
        18    50328.      0.200339064               2258
        20    50328.      0.20021084               2254
beam impedance= (-6739.99414,8301.81152)
cavity impedance= (0.0173392985,-39.8967094)
matched cavity impedance= (2032.10547,13506.2148)
drive power required is   150357.313watts
matched drive is  2.89626217watts
with loaded q of  79.6204987and frequency  2.87186227E+009
cavity    voltage   induced current   harmonic current  efficiency
 1         288.0000        0.0027        0.0000        0.0000
 2        8300.0000        0.0202        0.0000       -0.0016
 3       21356.0000        0.1921        0.0000        0.0406
 4       50328.0000        0.4017        0.0000        0.2002
```

Figure 3.8: KLYNAC output file for cavity separations equal to a half wavelength of the propagating mode $f = 2.856$ GHz.

The efficiency of the previous result was pretty good, but we still wanted to reach more and we had understanding that it is possible. The beam speed is not exactly half of the speed of light at the entrance; it is modified in the process and not the same for different particles. In addition, the output cavity has to extract power from the electron beam; hence, the proper synchronism should be maintained different from the one in previous cavities.

Based on these facts we modified distances and voltages to find an optimum configuration (Fig. 3.9) delivering an efficiency of 42% (Fig. 3.10). In this step two "idler" cavities compensate each other and huge positive efficiency in the output cavity is observed. After

this design configuration was determined we added a field mapping in each cavity to make it closer to the real-life configuration, as described in the next section. At that time the power balance equation had not been analyzed yet and we did not have in mind the other structure, where the last cavity is uncoupled. However, it seems to us more logical, first, to describe the difference of building the type-2 design in that configuration without mapping, taking into account the fact that not a lot of modifications from the design described above were required.

```
2.856e9 50.e+3 10.0 0.01 .28 300 11 281 1 4
4 2. 2  +1  1 11
.066e-2
4 3  20
0.005  0.78 2.0
.002 .0 .0 .0
0.248 .0 .0 .011:18 04.09.2016

1  (6900.,0.)    .045  .018  7.0e8    153.  600.
1  (-11100.,0.)  .121  .018  7.05e8   153.  700.
1  (23500.,0.)   .175  .018  7.27e8   153.  1200.
1  (-72000.,0.)  .225  .018  7.35e8   153.  1200.
```

Figure 3.9: KLYNAC input file for the optimum configuration for type-1 structure.

```
        18    72000.      0.421487093                2434
        20    72000.      0.4208785                 2428
beam impedance= (-28662.8242,6317.06738)
cavity impedance= (0.0173392985,-39.8967094)
matched cavity impedance= (63186.1836,42520.5586)
drive power required is   85857040.watts
matched drive is  1051.36011watts
with loaded q of  118.705032and frequency  2.85760205E+009
cavity    voltage   induced current   harmonic current  efficiency
 1        6900.0000        0.0235        0.0000       -0.0016
 2       11100.0000        0.3493        0.0000       -0.0369
 3       23500.0000        0.4747        0.0000        0.0299
 4       72000.0000        0.6853        0.0000        0.4209
```

Figure 3.10: KLYNAC output file for the optimum configuration for type-1 structure.

3.2.2 Uncoupled output cavity

For the type-2 structure the output cavity voltage phase was a free parameter which gave us the opportunity to get more efficiency from the klystron part than before. An alternative option for the free parameter is to fix the distance between the last coupled cavity and the output cavity to satisfy some actual design needs and then adjust the phase to reach maximum efficiency . One may ask why more efficiency is necessary once we have already achieved a result close to 50%. However, once we added some real cavity geometries and field mapping, as explained in the next section, the efficiency decreased. In this case, changing cavity position and adjusting the voltage are not exactly equal procedures and phase freedom as an extra parameter in the output cavity will help a lot.

Similarly for any type of structure, once the desired efficiency is reached we have to hope that these voltage amplitude ratios can be realized for a given gap size and cavity separation in a real 3D geometry with appropriate coupling coefficients. However for the type-2 structure it is easier to do since only first three cavities are coupled to each other. Furthermore, to make our design more realistic, initially for the type-1 structure and eventually for type-2, we had to add real cavity geometry and actual field mapping in KLYNAC code simulations instead of using the gridded gap model.

3.3 Using real cavity geometry

Poisson Superfish is a great tool to obtain field mapping for a given cavity geometry. Based on the idea that $\pi/2$ mode does not drive coupling cavities, we initially created the mapping only for the klystron cavities, leaving coupling cells as drift sections in our simulations. We will present the simulation results at the end of this chapter discussing

competing modes for a real mapping in all the cavities and it will be clear that for our main mode we do not need any mapping inside the coupling cells as supposed. Initially, we started with a very simple sphere-type geometry (Fig. 3.11, on the left).

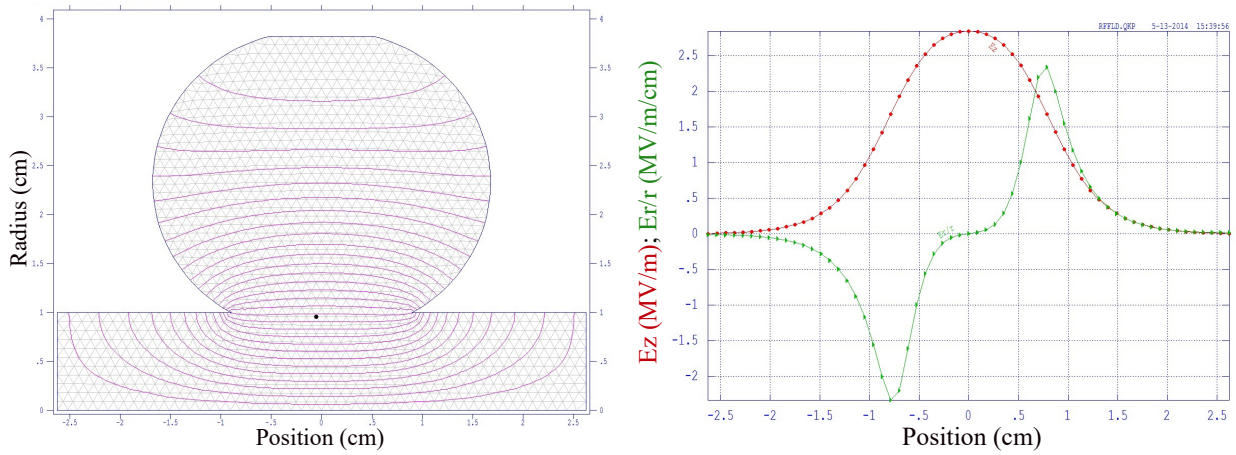

Figure 3.11: Superfish electric field lines (left) and electric field dependence (right) for simple spherical cavity geometry.

Playing with characteristic scales we got the desired resonance frequency. To do that, we used a big mesh first to run Superfish faster, and once we found the necessary parameters we decreased the mesh size to have a more detailed mapping of the field (Fig. 3.11, on the right). Using the derived field map we ran KLYNAC simulations for the klystron part with all the previous settings (Fig. 3.12) and observed significantly smaller efficiency (Fig. 3.13). We did a little bit of tuning of cavity voltages and positions to maximize the Klynac efficiency but did not spend too much time on it since better cavity configurations exist.

```
1  (6900.,0.)    .045   -.018  7.0e8     153.   600.
sphere7.t7
1  (-11100.,0.)  .121   -.018  7.05e8    153.   700.
sphere7.t7
1  (23500.,0.)   .175   -.018  7.27e8    153.   1200.
sphere7.t7
1  (-72000.,0.)  .225   -.018  7.35e8    153.   1200.
sphere7.t7
```

Figure 3.12: KLYNAC input file with adding real field mapping for the specific geometry. The negative sign of the gap means adding mapping, while the actual map is located in the file sphere7.t7.

```
         18    72000.      0.169962361                4351
         20    72000.      0.169959933                4351
beam impedance= (-26989.5996,-14934.8955)
cavity impedance= (0.0173392985,-39.8967094)
matched cavity impedance= (29817.4824,-42990.2617)
drive power required is   85699296.watts
matched drive is  934.557495watts
with loaded q of  130.357437and frequency  2.85257062E+009
cavity    voltage   induced current   phase of Iind  efficiency
 1        6900.0000        0.0224        2.6362       -0.00135049
 2       11100.0000        0.1638       -0.3687       -0.01695749
 3       23500.0000        0.2230       -1.3859        0.00963811
 4       72000.0000        0.5313       -2.0311        0.16995993
electronic efficiency is  1.
current transmission is  0.
```

Figure 3.13: KLYNAC output file for the structure with spherical cavities. Adding real mapping lowers the efficiency of the klystron part.

Next, we used the cavity geometry (Fig. 3.14, on the left) from the previous work by Schriber [23], tuned its frequency to 2.856 GHz, and obtained the results (Fig. 3.14, on the right; Fig. 3.15) by using the same input parameters as before. The efficiency was much better than in the previous geometry but still smaller than in 1D case. We decided to play with this cavity shape slightly to see if it would result in significant changes. We repeated the same procedure for the modified geometry (Fig. 3.16, on the left) and observed a tiny bit better results (Fig. 3.16, on the right; Fig. 3.17). However, the previous type is more popular and cheaper to realize while the efficiency is about the same. Therefore, we did more

re-optimization of the cavity voltage amplitudes and positions to maximize the efficiency of the klystron with the second type field map. For the all-coupled cavities design (Fig. 3.18) we got overall efficiency of 42% (Fig. 3.19), whereas for the type-2 structure the optimum configuration can potentially deliver better results. We did not do separate optimization for only the klystron part for the type-2 structure, but we will present the result of an optimum structure for the whole Klynac in the next section.

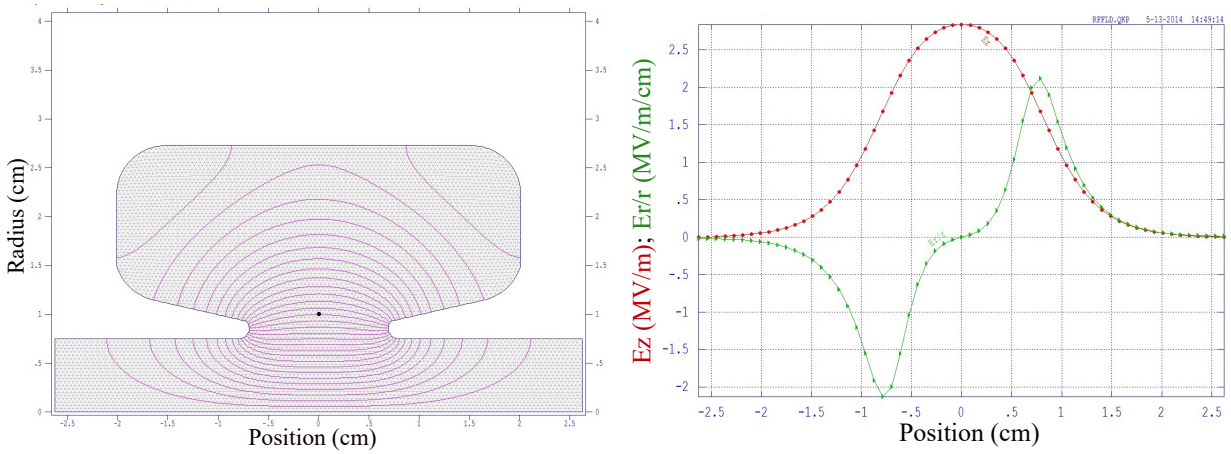

Figure 3.14: Superfish electric field lines (left) and electric field dependence (right) for the realistic cavity geometry.

```
        18    72000.      0.352616012                4802
        20    72000.      0.352618128                4802
beam impedance= (-32457.2227,-940.321533)
cavity impedance= (0.0173392985,-39.8967094)
matched cavity impedance= (91188.9609,-7464.56934)
drive power required is   85800680.watts
matched drive is  992.125549watts
with loaded q of  124.327408and frequency  2.85580518E+009
cavity    voltage   induced current   phase of Iind  efficiency
 1        6900.0000        0.0212        3.1126       -0.00146562
 2       11100.0000        0.2960       -0.1727       -0.03236436
 3       23500.0000        0.4961       -1.1704        0.04544341
 4       72000.0000        0.8073       -2.2226        0.35261813
```

Figure 3.15: KLYNAC output file for the structure, where cavities are realized in 3D using realistic model. Mapping with realistic cavity geometries delivers bigger efficiency of the klystron part than using a simplified model but still smaller than in no mapping case.

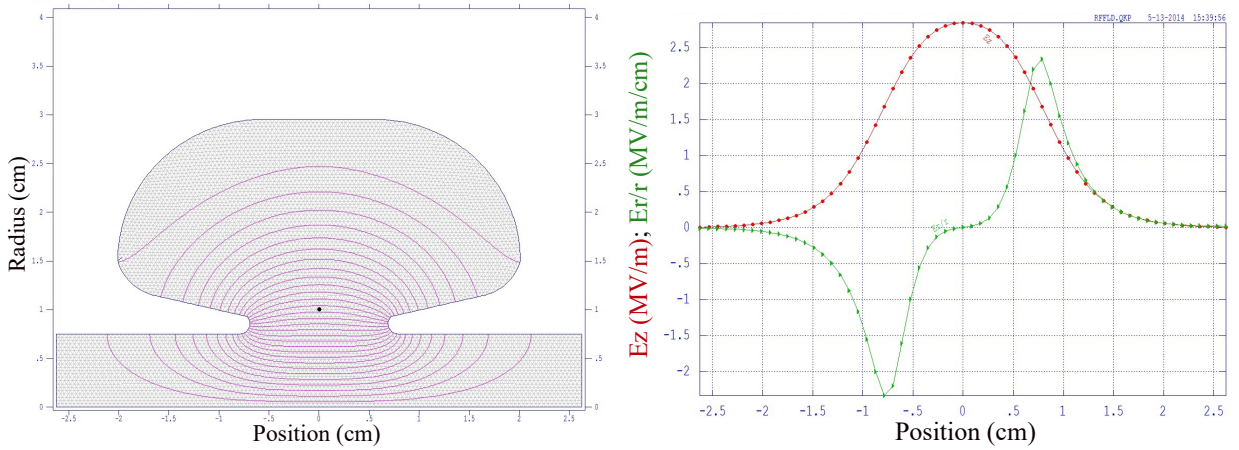

Figure 3.16: Superfish field lines (on the left) and field dependence (on the right) for the alternative cavity geometry.

```
         18    72000.      0.353424847                4809
         20    72000.      0.353422552                4810
beam impedance= (-32506.6719,-853.326782)
cavity impedance= (0.0173392985,-39.8967094)
matched cavity impedance= (91298.5156,-6766.42676)
drive power required is   85801264.watts
matched drive is  991.120667watts
with loaded q of  124.427414and frequency  2.85582362E+009
cavity    voltage   induced current   phase of Iind  efficiency
 1        6900.0000        0.0212        3.1153       -0.00146361
 2       11100.0000        0.2967       -0.1719       -0.03244858
 3       23500.0000        0.4977       -1.1694        0.04569779
 4       72000.0000        0.8082       -2.2236        0.35342255
```

Figure 3.17: KLYNAC output file for the alternative geometry mapping. Results are very similar to the typical realistic geometry presented before.

We suggest anyone, who will design a Klynac-like device for a specific application, should study the question of an optimum geometry in more detail, taking into account that such a geometry should satisfy the $\pi/2$ mode configuration, but we left it to James Potter to decide what specific geometry of a klystron cavity we would have in our prototype. He designed it very similar to the second type we used here. Later we built it for our Klynac prototype device.

```
2.856e9 50.e+3 10.0 0.0075 0.4 300 16 801 0 8  3.14
12 2. 2  +1  1 31
0 0
1560 1620 0
4 4  20
0.005 0.69 0.02
.002 .0 .0 .0
0.248 .0 .0 .0


1  (11100.,0.)   .045  -.018  7.0e8    153.  600.
sphere8.t7
2  (-12100.,0.)  .120  -.018  7.05e8   153.  700.
sphere8.t7
3  (24500.,0.)   .1735  -.018  7.27e8   153.  1200.
sphere8.t7
4  (-86000.,0.)  .2255  -.018  7.35e8   153.  1200.
sphere8.t7
```

Figure 3.18: KLYNAC input file for the optimum structure configuration, where mapping is calculated for the typical cavity geometry.

Since we added real field maps in our simulations, we got some transverse dynamics imposed by E_r in the cavities, in addition to one we had before, caused by the space charge forces. We studied manipulations on the transverse beam dynamics via piece-wise linear magnetic field B_z provided by solenoid along the device as it was initially proposed by James Potter et al. [12]. Applying variable focusing elements (for example, non-uniform solenoid) for transverse beam dynamics correction can significantly increase the efficiency of the system and prevent the beam from spreading and hitting the walls completely. However, in the built prototype we only have two solenoids with a uniform magnetic field profile. First solenoid is placed on the exit of the electron gun, and second one is covering the klystron section. Therefore, all transverse beam dynamics in the accelerator sections are controlled by these two solenoids and an aperture. In our final simulations we ended up with a uniform magnetic field along the structure.

```
         18    86000.      0.38973543                4926
         20    86000.      0.389732271                4926
beam impedance= (-32486.3125,-988.917725)
cavity impedance= (0.0173392985,-39.8967094)
matched cavity impedance= (91126.875,-7831.98389)
drive power required is   222042944.watts
matched drive is  2565.65991watts
with loaded q of  124.399025and frequency  2.85579546E+009
cavity    voltage   induced current   phase of Iind  efficiency
 1       11100.0000        0.0342        3.1112       -0.00378916
 2       12100.0000        0.4401       -0.0580       -0.05315757
 3       24500.0000        0.6725       -1.0624        0.08019974
 4       86000.0000        0.7149       -2.2574        0.38973227
```

Figure 3.19: KLYNAC output file for the optimum structure configuration, where mapping is calculated for the typical cavity geometry. High-efficiency for the type-1 configuration is reached in realistic simulations.

After the mapping simulations part was done, Bruce Carlsten added a beam aperture mechanism in the KLYNAC code blocking the desired amount of the electron beam after the klystron part. It was realized simply by blocking radial cells at some longitudinal location, so the electrons were not able to travel through it and remained in the klystron part only. We were able then to start designing the accelerator part.

3.4 Designing accelerator part

3.4.1 Type-1

In this section, first we will explain how we designed the accelerator part for type-1 Klynac and then will add details about how it was modified for the type-2 structure. The initial design of the accelerator part started from optimizing an aperture size to reach desirable beam current. We planned on only 1% of initial current to go through. In the PIC code KLYNAC an aperture was realized the way that some desirable cells were blocked and

electrons were not able go through them. We made an assumption of cylindrical symmetry in the code, so our 3D particle dynamics code had 2D cell structure along the longitudinal coordinate and radius. Evolution of the beam in x and y were still different as you can see in Fig. 3.20: top left and top right respectively and on the bottom of the figure radial evolution is presented.

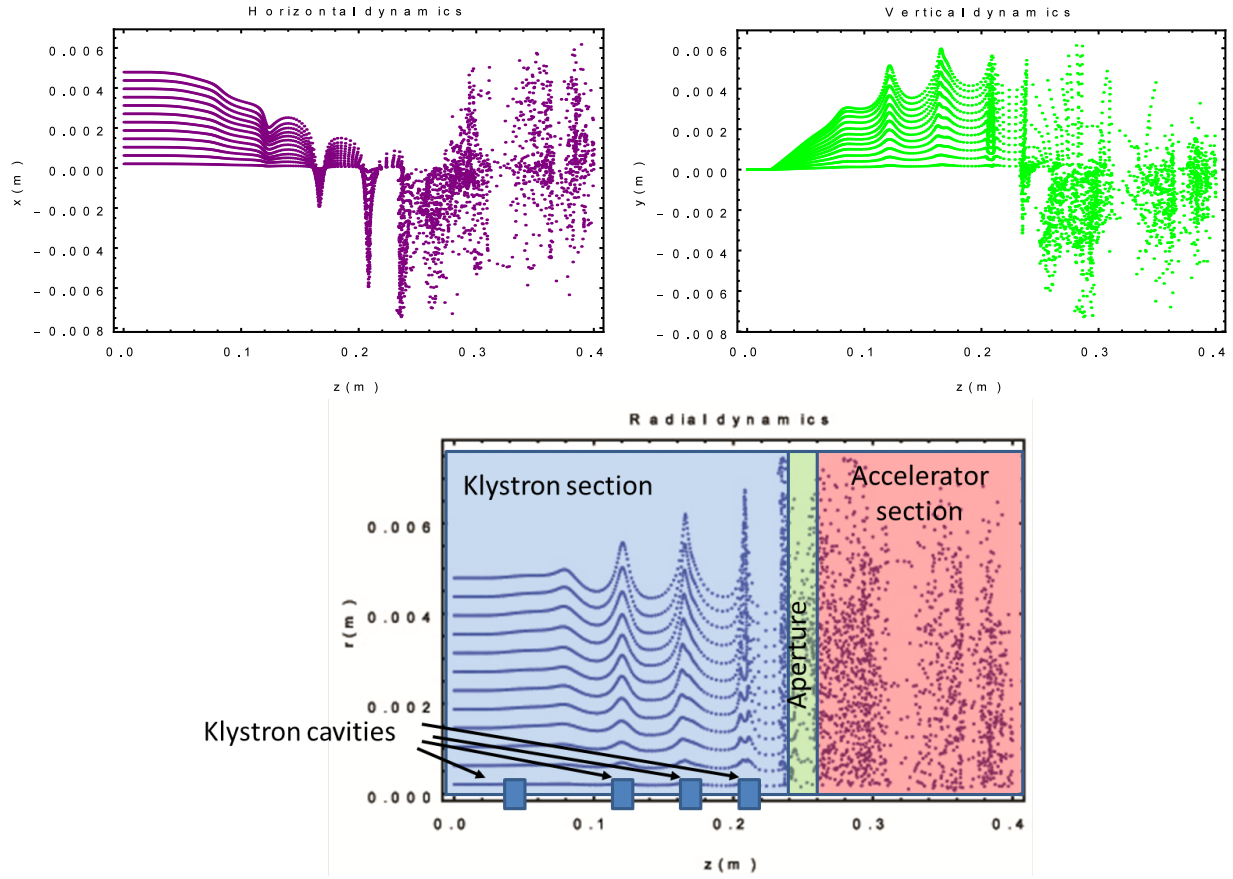

Figure 3.20: Particle dynamics in KLYNAC code is presented for klystron cavities and free space after them, as an example. Horizontal dynamics (on the left up) is different from the vertical dynamics (on the right up) for non-symmetric particle injection. For correct space charge calculations, symmetric injection is required, so the radial dynamics is presented (on the bottom). Regions of the Klynac are highlighted according to the scheme in Fig. 1.1.

The beam aperture was simulated as permanent in time; however, if one can think of a fast mechanical aperture, time evolution can be added for future applications. To control what

part of the beam goes through, we changed the amount of open cells in z and r directions. If an electron beam did not have any transverse dynamics, then obviously only radius size matters. As soon as we introduced transverse dynamics via real mapping in the cavities, longitudinal size as well as aperture position were important too. In the Fig. 3.21 we compare beam dynamics in the case of no aperture with two others of the same radial aperture but with different length. Evolution of $\gamma\beta_z$ for the no aperture and optimum aperture cases are represented on the top left and top right of Fig. 3.22 respectively.

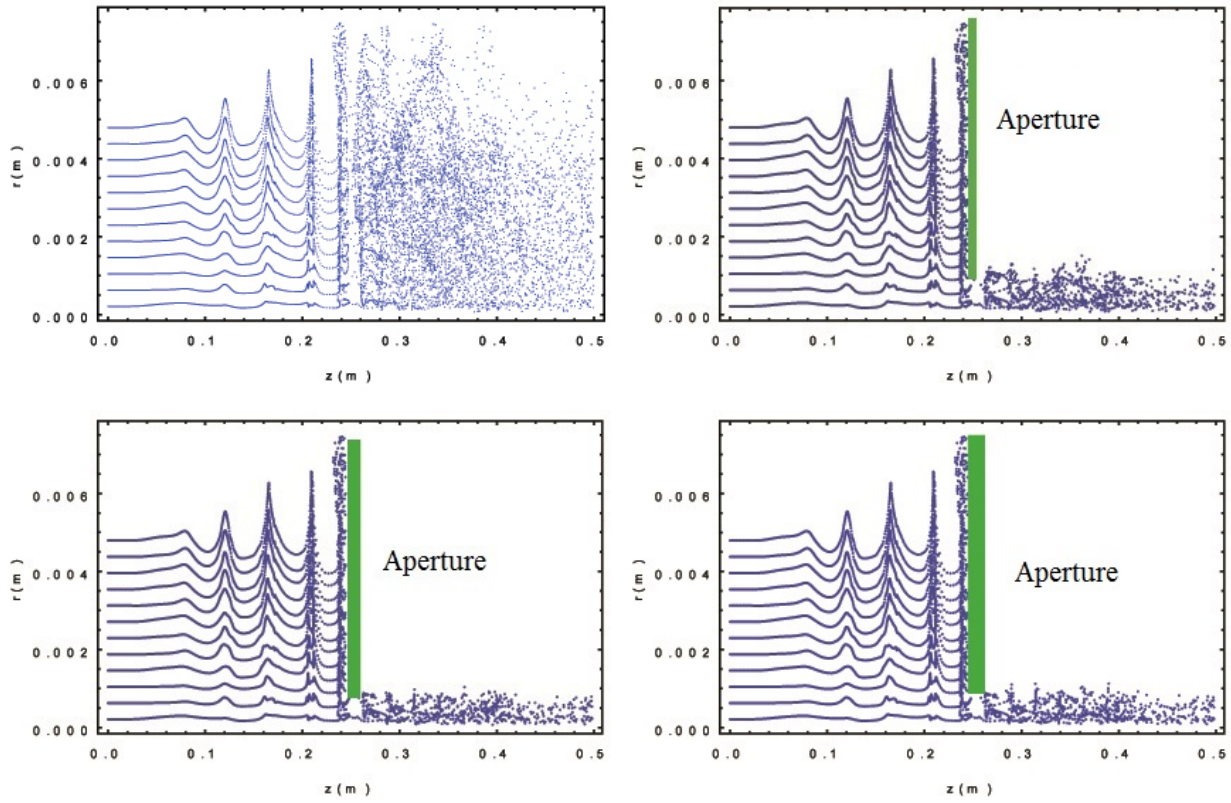

Figure 3.21: Radial dynamics for different apertures. On the top left, no aperture case; on the top right, inserting the beam stop with an aperture; on the bottom left, changing the beam dump length leaving the radial aperture size the same; on the bottom right, an optimum aperture delivering 1% of a beam to go through.

Arbitrary combinations of r and z cells can result in the necessary percentage of the beam going through. We picked the combination which gave us good transverse dynamics in the

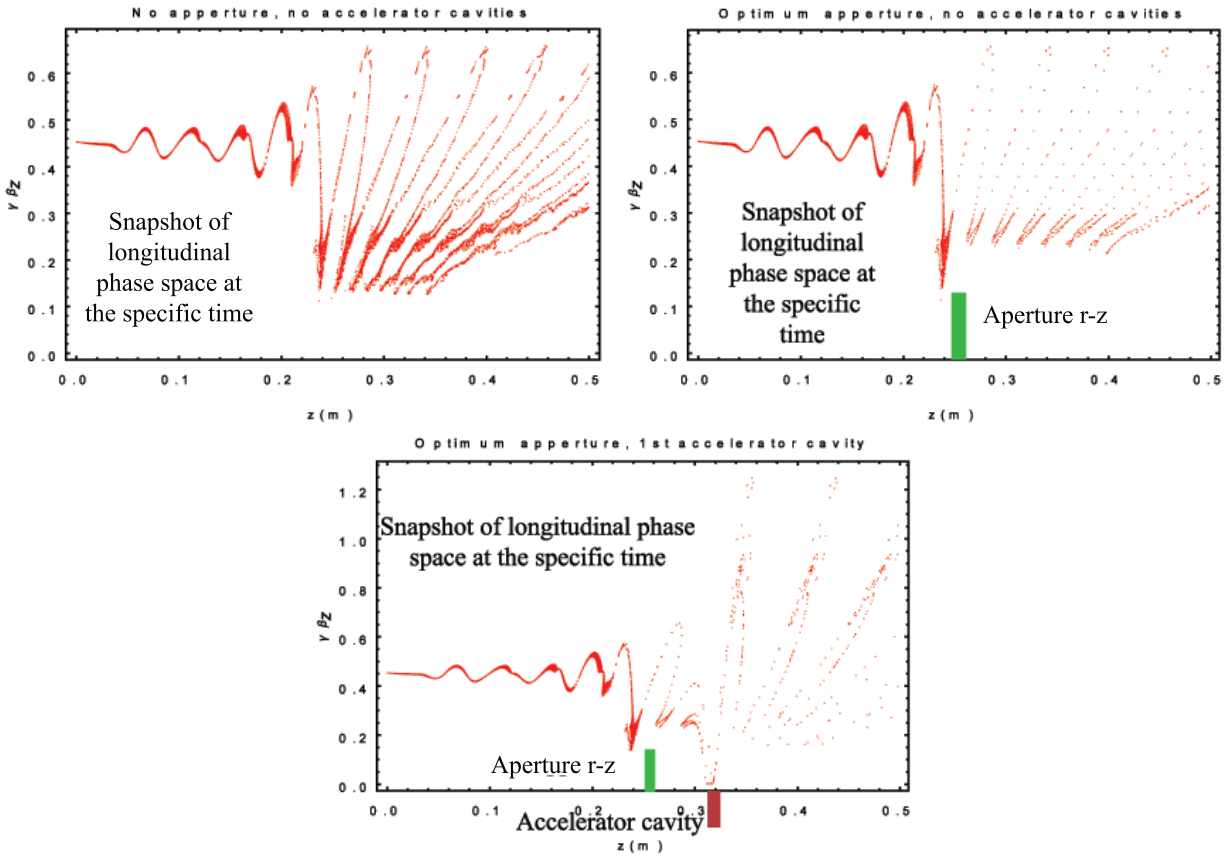

Figure 3.22: Normalized energy behavior for the different configurations of the accelerator section. The case of no aperture and no accelerating cavities is presented on the top left, the case of the optimum aperture and no accelerating cavities on the top right, adding the first accelerator cavity to the optimum aperture configuration on the bottom.

accelerator part. In addition, to make the aperture more precise, one may need to increase the amount of cells in both directions as well as the number of particles, which certainly would increase the time of running simulations. By the overall length of the system and amount of cells, the longitudinal cell size was defined. Analogically, by maximum radius size and amount of radial cells, transversal size was defined. For instance, in the type-1 design we reached a desired percentage of the beam going through and good traverse dynamic via blocking 26 from a total of 30 cells at the longitudinal locations from 490 to 550, while total amount of z cells was 1000 and total length 0.5 m (Fig. 3.21 right-down corner).

Opened radial cells were close to the radius and had rectangular geometry. In principle, the input file can be modified without significant modifications of the code to open cells not on the axis and make the aperture of an arbitrary shape for some purposes .

As it is realized in a typical accelerator structure, we decided to have the same amplitudes in all accelerating cavities. Our goal was to reach a beam energy of 1 MeV, so four accelerator cavities with 250 kV amplitudes would be enough. Of course, we were planning to run it in $\pi/2$ mode, which means the π shift between neighbors. In the region where electron beam would reach the relativistic regime, distances between cavities would be locked to 5.25 cm (half wavelength for f=2.856 GHz). The gap size had to be the same as for the klystron cavities to simplify the design. The only undefined parameters for the type-1 structure after we set up the aperture were the location of the first two accelerating cavities (0.5 MeV $\sim \gamma = 2 \sim \beta = 1.7$). The first cavity position search was not straightforward. In opposite to the patent authors' idea of picking the high-energy beam part, we desired to pick a bunch with less energy but better quality. As you can see in the center of Fig. 3.22, there are some low-energy electron bunches at some z positions as well as some high-energy particles between them. Under some specific realization of an aperture there will be enough high-energy particles to accelerate them further. However it might be tricky to construct because the energy difference is not significant at that stage yet. In addition, it is important to exclude extra particles from the propagation in the accelerator section. Therefore, we wanted to put the first accelerating cavity in one of the spots where the electron beam was concentrated with a small energy spread. On the second step we adjusted the cavity position, slightly maximizing the output energy of the beam. The second cavity position was found by optimizing the output $\gamma\beta_z$ as well, taking into account that travel distance should be still smaller than 5.25 cm.

The final design for the type-1 structure is represented on the left of Fig. 3.23. Simulation results of $\gamma\beta_z$ and radial evolution are on the left and right of Fig. 3.24 respectively. We

reached the desired energy ~ 1 MeV $\sim \gamma\beta_z = 2$. This design required around 2.6 kW of input RF power driving the beam defined by the first cavity voltage ($\sim V^2$) and beam parameters but had really good efficiency. We designed an alternative version with 30% efficiency but required only 40 W input power (Fig. 3.23, on the right) and were almost ready to start realizing it in 3D geometry when we figured out a Klynac realized as an all-coupled structure would not work for given parameters as we discussed in Chapter 2. This type of the design took approximately six months to create and the understanding that it would not turn on came to us in the last minute. However, we gained a lot of knowledge about how to do the simulation design, so it took us less than two weeks to come up with a new design satisfying the type-2 structure.

```
2.856e9 50.e+3 10.0 0.0075 0.75 600 31 1501 1 8  3.14
12 2. 2  +1  1 31
4.75e-2 0
490 550 26
8 8  12
0.005 0.69 0.02
.002 .0 .0 .0
0.248 .0 .0 .0
1  (11200.,0.)   .045  -.018  7.0e8    153.  600.
sphere8.t7
2  (-12100.,0.)  .121  -.018  7.05e8   153.  700.
sphere8.t7
3  (25000.,0.)   .176  -.018  7.27e8   153.  1200.
sphere8.t7
4  (-86000.,0.)  .227  -.018  7.35e8   153.  1200.
sphere8.t7
5  (250000.,0.)  .315  -.018  7.35e8   153.  1200.
sphere8.t7
6  (-250000.,0.)  .3475  -.018  7.35e8   153.  1200.
sphere8.t7
7  (250000.,0.)  .4  -.018  7.35e8   153.  1200.
sphere8.t7
8  (-250000.,0.)  .4525 -.018  7.35e8   153.  1200.
sphere8.t7
```

```
beam impedance= (-32362.8105,-1447.66101)
cavity impedance= (0.0173392985,-39.8967094)
matched cavity impedance= (90351.6953,-11439.2793)
drive power required is   226053760.watts
matched drive is  2617.3811watts
with loaded q of  124.199738and frequency  2.85569869E+009
cavity    voltage   induced current   phase of Iind  efficiency
 1       11200.0000        0.0346        3.0969       -0.00386831
 2       12100.0000        0.4209       -0.3032       -0.04860927
 3       25000.0000        0.5673       -1.5332        0.00533666
 4       86000.0000        0.6949       -2.5374        0.49182075
 5      250000.0000        0.0206        2.4027       -0.03799336
 6      250000.0000        0.0221       -0.1802       -0.05437694
 7      250000.0000        0.0212        2.2438       -0.03298822
 8      250000.0000        0.0120       -1.2641       -0.00904470
```

```
2.856e9 50.e+3 10.0 0.0075 0.8 600 31 1601 1 8  3.14
12 2. 2  +1  1 31
4.75e-2 0
560 620 28
8 8  12
0.005 0.69 0.02
.002 .0 .0 .0
0.248 .0 .0 .0
1  (1500.,0.)   .097  -.018  7.0e8    153.  600.
sphere8.t7
2  (-12100.,0.)  .148  -.018  7.05e8   153.  700.
sphere8.t7
3  (14000.,0.)   .211  -.018  7.27e8   153.  1200.
sphere8.t7
4  (-72000.,0.)  .261  -.018  7.35e8   153.  1200.
sphere8.t7
5  (250000.,0.)  .340  -.018  7.35e8   153.  1200.
sphere8.t7
6  (-250000.,0.)  .3725  -.018  7.35e8   153.  1200.
sphere8.t7
7  (250000.,0.)  .4250  -.018  7.35e8   153.  1200.
sphere8.t7
8  (-250000.,0.)  .4775 -.018  7.35e8   153.  1200.
sphere8.t7
```

```
beam impedance= (-36481.7969,-1778.41846)
cavity impedance= (0.0173392985,-39.8967094)
matched cavity impedance= (90444.6953,-11071.6025)
drive power required is   4054705.75watts
matched drive is  43.0190926watts
with loaded q of  133.027267and frequency  2.85570867E+009
cavity    voltage   induced current   phase of Iind  efficiency
 1        1500.0000        0.0041        3.0929       -0.00006153
 2       12100.0000        0.0071       -1.5173       -0.00004602
 3       14000.0000        0.3286       -1.5690        0.00008359
 4       72000.0000        0.4894       -2.5958        0.30119026
 5      250000.0000        0.0037        2.7600       -0.00852550
 6      250000.0000        0.0042        0.0474       -0.01055648
 7      250000.0000        0.0040        2.5423       -0.00821088
 8      250000.0000        0.0037       -0.7321       -0.00680536
```

Figure 3.23: Optimum klystron design for the type-1 structure. The first configuration requiring 2.6 kW delivers around 50% efficiency (on the left) and second configuration requiring only 40 W of input power delivers 30% efficiency (on the right).

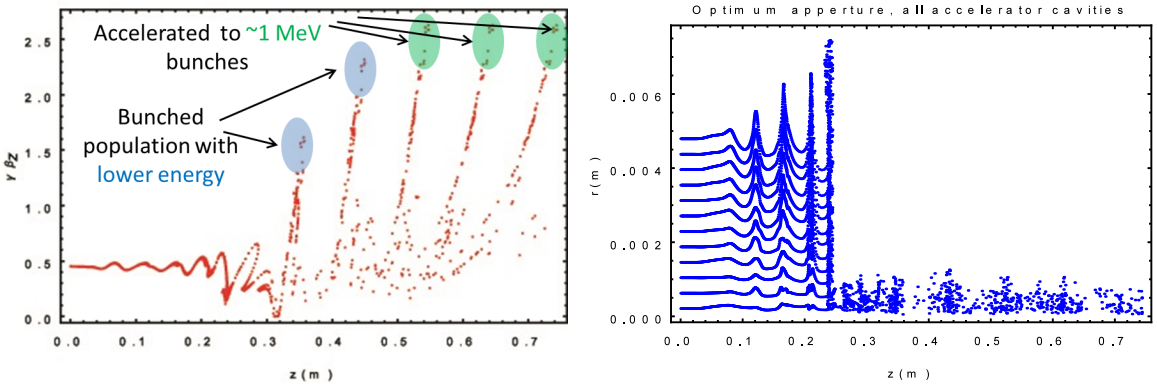

Figure 3.24: Beam dynamics for the optimum klystron type-1 structure is presented. Normalized energy dependence from the longitudinal coordinate on the left and radial dependence on the right.

3.4.2 Type-2

Initially, once we designed the klystron part we had an understanding that it would be easier to get high-efficiency in the klystron part because of an extra free parameter. Our goal was to keep stability of the scheme and increase efficiency. In the accelerator part we would have to follow the phase which we set up in the output klystron cavity by adding π shift to it on each accelerating cavity. We came up with a design (Fig. 3.25) delivering 40% efficiency (more than previous one) and requiring around 1kW of input power. The beam dynamics is presented on Fig. 3.26.

We had an appropriate TWT source at our experimental facility working at the time we made our design. After the Klynac was built, we started the experimental setup, tested that source, and realized it does not actually work. The only alternative source we have at the moment is another TWT with maximum of 250 W power only. Cavity voltages in this case have to be re-scaled about factor of two, which will dramatically change the efficiency of the scheme to 13% as well as beam dynamics (Fig. 3.27). An alternative option to get good results with smaller power source is to reduce current of the beam. If one lowers it from 10 A

to 1 A, then only around 400 W of power is required to maintain voltages on the appropriate level. Efficiency stays around 40% and $\gamma\beta_z$ dynamics almost does not change while radial dynamics changes can be fixed by magnetic field adjustment (Fig. 3.28). We have to admit that to test our Klynac prototype we have to have an input source with variable frequency, so we can actually drive our device on its real frequency, which can be different from what we designed it for, so to drive our device with a klystron at this point is not an option. We still hope that the original input source will be fixed or we will find an appropriate alternative.

```
2.856e9 50.e+3 10.0 0.0075 0.8 600 31 1601 1 1  3.14
12 2. 2  +1  1 31
4.75e-2 0
500 520 27
8 8  12
0.005 0.69 0.02
.002 .0 .0 .0
0.248 .0 .0 .0
1  (7500.,0.)   .045  -.018  7.0e8    153.  600.
sphere8.t7
2  (-9937.,0.)  .108  -.018  7.05e8   153.  700.
sphere8.t7
3  (40400.,0.)   .1695  -.018  7.27e8   153.  1200.
sphere8.t7
4  (72500.,-43000.)  .1995  -.018  7.35e8   153.  1200.
sphere8.t7
5  (-215051.,127551.)  .283  -.018  7.35e8   153.  1200.
sphere8.t7
6  (215051.,-127551.) .3130  -.018  7.35e8   153.  1200.
sphere8.t7
7  (-215051.,127551.)  .3655  -.018  7.35e8   153.  1200.
sphere8.t7
8  (215051.,-127551.)  .4180 -.018  7.35e8   153.  1200.
sphere8.t7
```

```
        12    250032.375     -0.00956527889                51026
beam impedance= (-32677.416,-1433.10876)
cavity impedance= (0.0173392985,-39.8967094)
matched cavity impedance= (90432.9375,-11118.8047)
drive power required is   101367680.watts
matched drive is  1165.40649watts
with loaded q of  124.898804and frequency  2.85570739E+009
cavity    voltage   induced current   phase of Iind  efficiency
 1        7500.0000        0.0229        3.0978       -0.00171807
 2        9937.0000        0.2283        1.4091       -0.00365391
 3       40400.0000        0.5292       -1.5345        0.00775048
 4       84292.6484        0.6967        0.2746        0.40495139
 5      250032.3750        0.0100       -1.3360       -0.01740128
 6      250032.3750        0.0115        2.4655       -0.02838689
 7      250032.3750        0.0104       -1.3683       -0.01757052
 8      250032.3750        0.0099        1.4323       -0.00956528
electronic efficiency is  1.
current transmission is  0.
```

Figure 3.25: KLYNAC input file for the optimum structure of the type-2 configuration on the left and output for it on the right showing 40% overall efficiency.

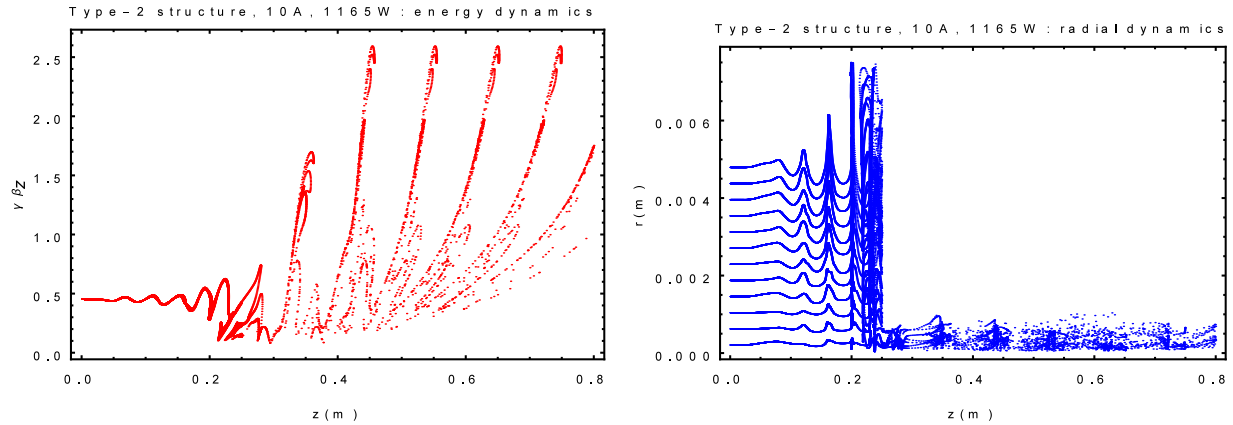

Figure 3.26: Beam dynamics for the optimum klystron type-2 structure is presented. Normalized energy dependence from the longitudinal coordinate on the left and radial dependence on the right. Results look slightly different from ones for the type-1 structure but in general the same dynamics delivering proper acceleration are observed.

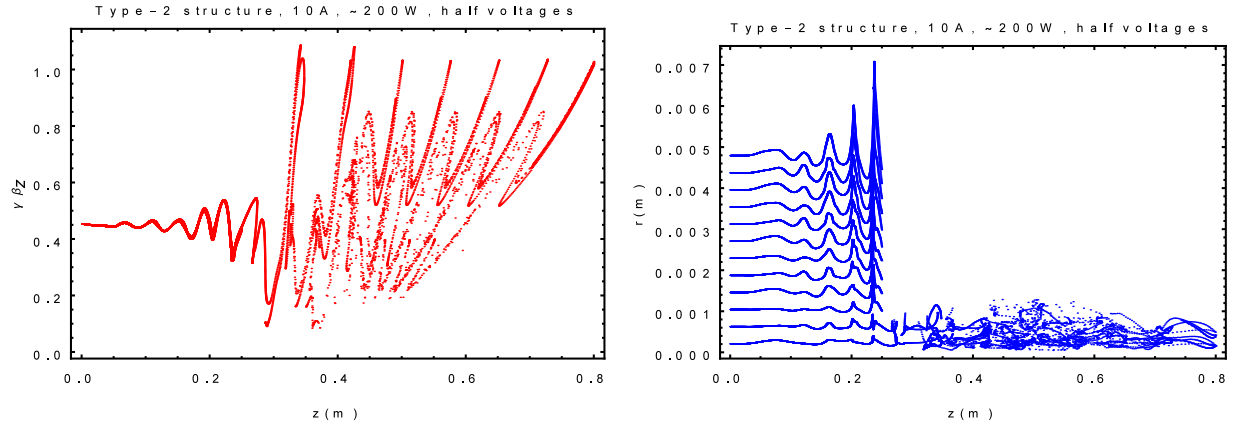

Figure 3.27: Beam dynamics for the optimum klystron type-2 structure with voltages rescaled by factor of two to match with 200 W input source instead of initially planned 1 kW source. Beam is not reaching the proper energy due to smaller voltages in the accelerator section (on the left); radial dynamics is not significantly impacted by voltages proration (on the right).

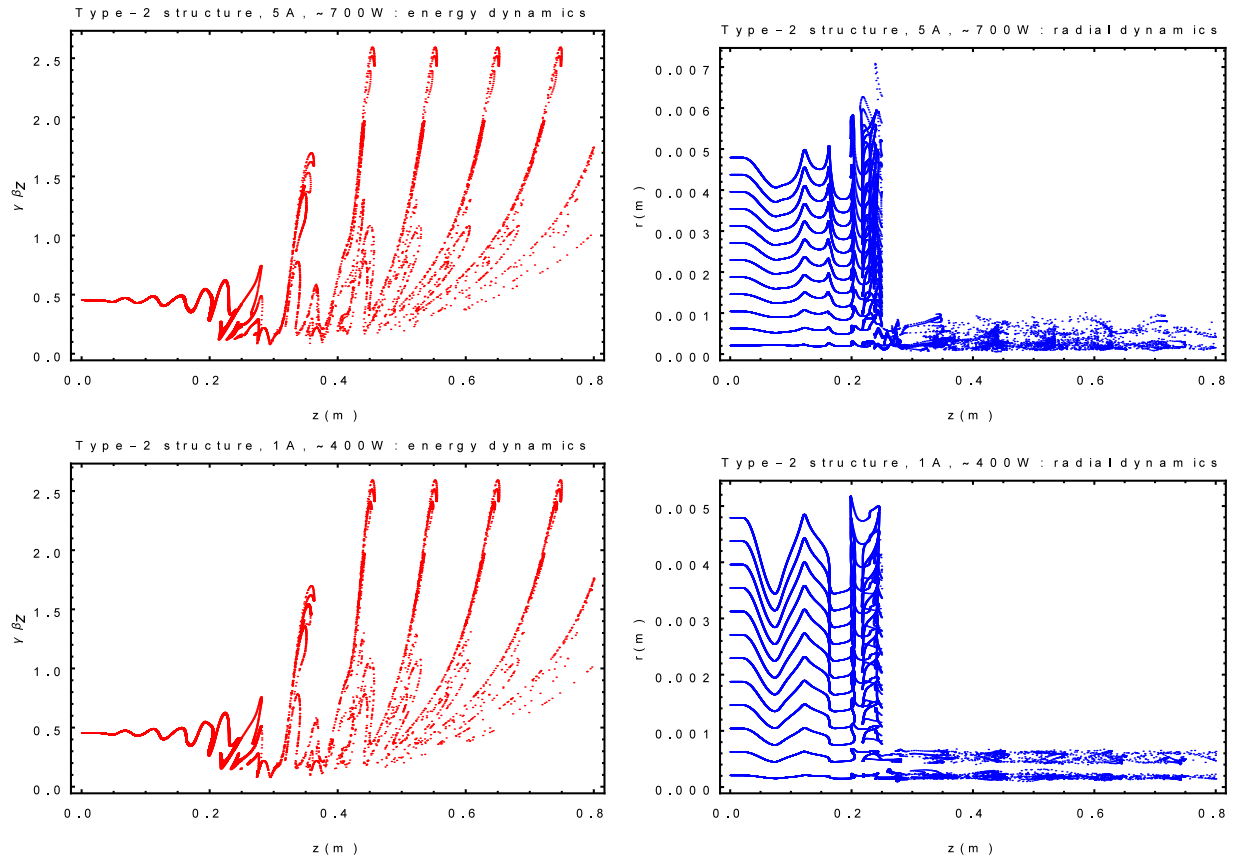

Figure 3.28: Beam dynamics (normalized energy dependence from the longitudinal coordinate on the left and radial dependence on the right) is presented for the optimum klystron type-2 structure with reduced current 5 A (on the top) and 1 A (on the bottom) to lower the required input power from 1.1 kW to 700W and 400W respectively.

3.5 Competing modes analysis

Once the actual prototype has been designed and built the simulation methods still remain a powerful instrument, mostly to understand the physics of what is going on, why and what we can do to change the behavior of a system. We realized that it might be interesting to check the competing mode behavior in the actual built prototype (Fig. 3.29). Once one has a geometry of the structure, eigen frequencies and eigen modes can be found analytically as described at the end of the previous chapter, numerically or even experimentally if the device has been built and there is a chance to do some cold testing. "Cold" means testing the structure with no beam in it and this technique is widely used to tune individual cavities, coupling slots and the whole structure in general [24]. In opposite "hot" testing means performing measurements in a structure with an electron beam in it. The electron beam can potentially load the structure. It can be interpreted as an electromotive force source with an internal impedance which affects the total impedance of the cavities, its quality factors and resonant frequencies.

We added real cavity geometries mapping for the coupling cells using the design numbers. In addition, we changed the geometry of the klystron cavities based on the built prototype parameters. Finally, we tuned the frequency to the numbers from the cold testing results for each cavity. Once the structure was built, some adjustments were done by grinding the metal. So we adjusted our geometry according to that. Even if we did not use accelerating cavities for competing mode analysis, we added real geometry for them as well just in case for future simulations, which can be required to understand the experimental results of the actual built structure.

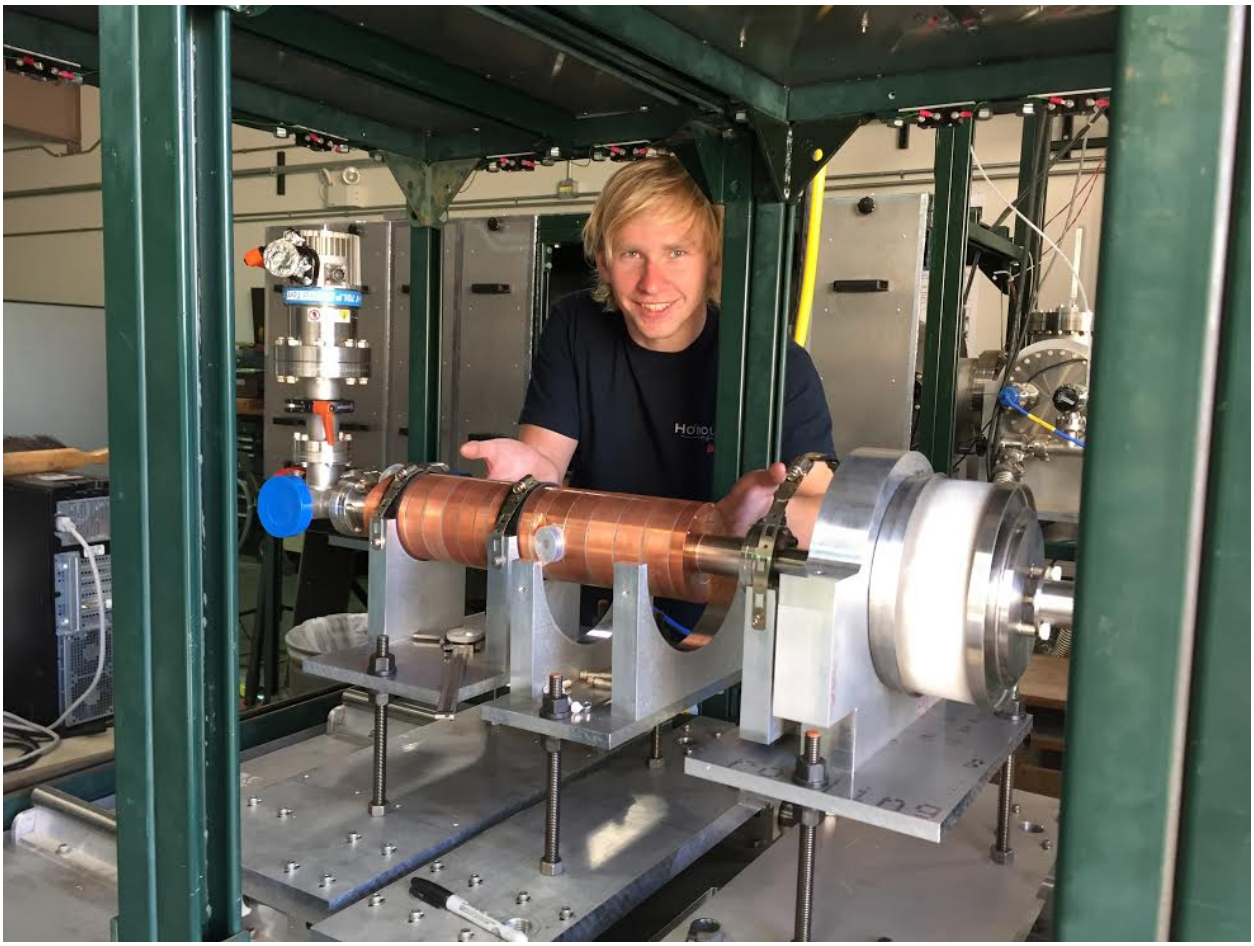

Figure 3.29: Built Klynac prototype. Alexander Malyzhenkov demonstrates a scale of the built Klynac prototype (bronze color tube) while it is not fully covered by an additional equipment of the experimental setup. Klynac is connected to the electron gun on the right and to the vacuum pump on the left.

James Potter provided us with eigen vector information. Using it we ran KLYNAC code to simulate in the first three cavities of the klystron part coupled to each other (type-2) for every mode separately. We limited our simulations to only three modes instead of five since 0 and $\pi/4$ modes are providing the same results as $3\pi/4$ and π respectively. The simulation results are represented for 0, $\pi/4$, $\pi/2$ on the top, in the middle and on the bottom of Fig. 3.30 respectively. We compare induced current at low voltages pro-scaled according to the eigen vectors for each mode satisfying 100 V voltage in the first cavity. Changing

the voltages in the first cavity (from 100 V - up) and changing accordingly voltages in the other cavities for each mode we can find the stability points for each mode. We can see that induced current is much bigger for $\pi/2$ mode in comparison to competing modes, which means these modes would not significantly change the dynamic of the Klynac we built from what we designed.

Competing modes analysis is an important step one should do in the process of designing a Klynac-like device. In the structure we built, we found the competing mode had no significant impact. Once the experimental setup is complete we will be able to check our theoretical estimate and simulation studies here for the competing mode influence on the beam dynamics and Klynac performance. However, simulation studies here confirm results of the theoretical estimate discussed in Chapter 2 of this thesis.

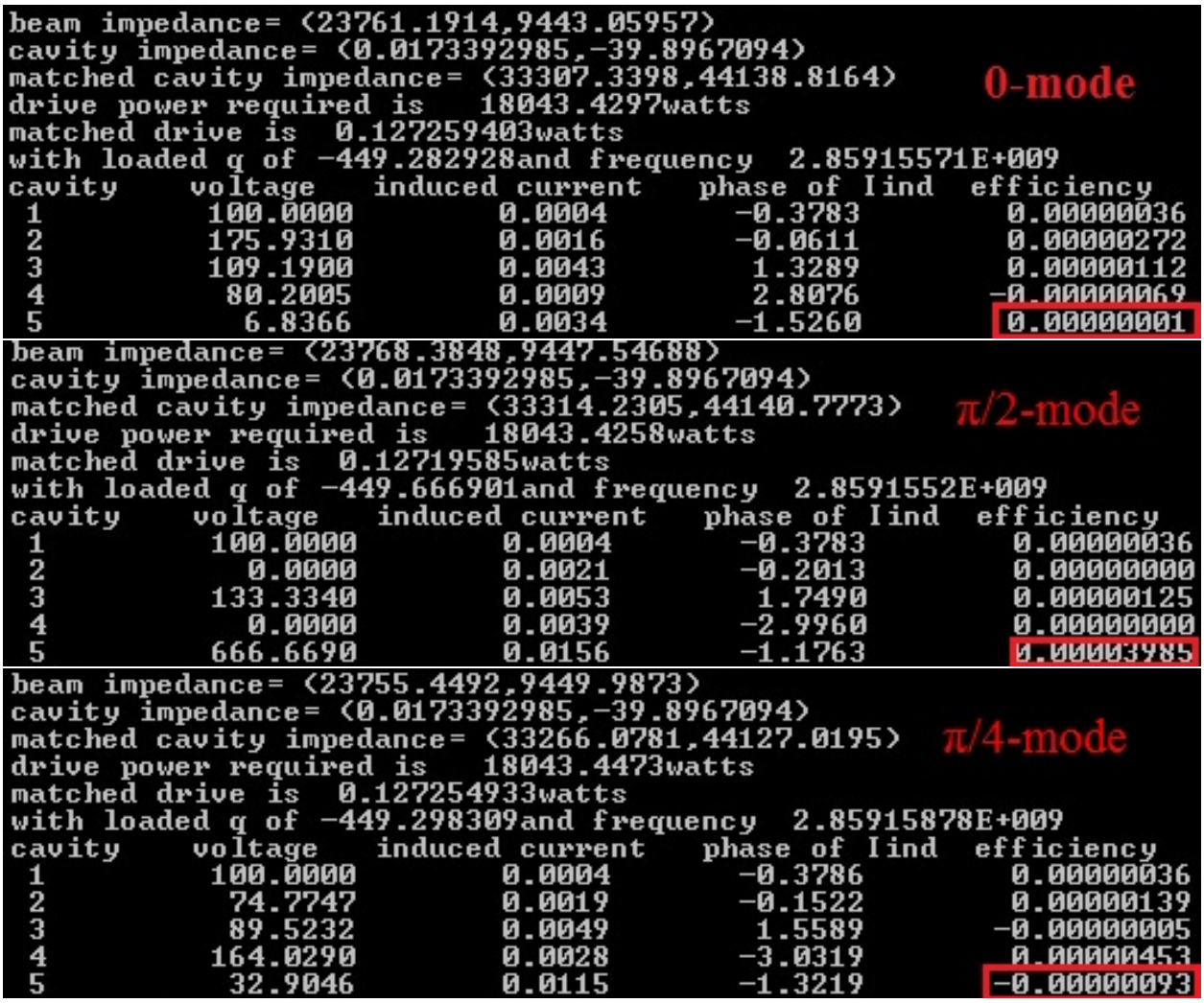

Figure 3.30: Simulations outputs for three competing modes. 0 on the top; $\pi/4$ on the bottom; main mode, $\pi/2$, in the middle. In these simulations coupling cavities are added in between of three first coupled cavities in the klystron section giving the total number of five coupling cavities, meaning five eigen modes competing with each other. However, only three of them are presented due to 0 and $\pi/4$ modes are providing the same results as $3\pi/4$ and π modes respectively, which is in strong agreement with a physical model. Comparing the overall efficiency (on the right-bottom corner of each output file) for each mode we make a conclusion that under similar initial conditions for all of them only main mode $\pi/2$ will build up. The comparison is done in the approximation of the similar eigen frequencies for each mode $f = 2.859$ GHz motivated by the single frequency of a driving source.

CHAPTER 4

CONCLUSION

In this chapter we first summarize the work what was done and described in this study for designing and building the Klynac prototype. The device we designed is, first of all, a proof of principles for a Klynac-like structure compact accelerator concept rather than a particular device for specific applications. Therefore, in the second part of this chapter we will scientifically fantasize about possible Klynac applications and specific geometries for some of them. Finally, we will conclude with a discussion of our future plans on the Klynac concept.

4.1 Results overview

At this moment the experimental tests of the prototype are on their way. Setting up the experiment together has unveiled unanticipated challenges. One of the main delays for the experiment was caused by a new electron gun. We had to solve the problem of heating the back side of the cathode which potentially could destroy our isolation transformer wire. We used an isolation transformer to deliver short impulse power to the gun. In addition, the transformer had arcs which destroyed our modulator internal modules. To prevent arcing we decided to fill the system with dielectric gas sulfur hexafluoride (SF6). This gas could not effectively help with dissipating heat associated with the cathode. Hence, additional water cooling of the cathode is required. In an ideal world one would like to do testing of the new prototype with the existing setup, but in our case it was completely another story.

We started this thesis with an overview of the previous ideas similar to the Klynac concept. Historically, not right away, but sometime after the work on the Klynac started, we found out that three patents were issued on the Klynac-like idea for a compact accelerator. We eventually appreciated that even if the concepts were patented, the actual device had never been built, and the proposed (patented) structure designs were, actually, concepts that needed significant work to be matured into a buildable design. Summarizing the above, we had a lot of work to be done before we started shaping the actual prototype parts in metal. One of the main unsolved problems for the Klynac-like device common to the all previous designs was practical realization of a coupler section, a section which has to transfer ideally all RF signal from the output klystron cavity and some small fraction of the electron beam.

In the beginning of the first chapter we discussed James Potter's idea for the coupler. He proposed resonantly connecting the output klystron cavity to the accelerator structure via an additional coupling cavity. Driving the device in $\pi/2$ would maintain no field in the last one and would support a power transfer with no loss. The geometry of such a cavity would have an aperture on axis, allowing only small fraction of the beam to go through.

After that we discussed Bruce Carlsten's idea on making Klynac device a single-resonant structure via coupling of all cavities in the klystron part and running the whole device in $\pi/2$ mode. We explained potential benefits (single mode, stability, no feedback, etc.) of such a configuration and introduced power balance analysis to understand if such a configuration can oscillate without any input power, strictly speaking, to build up a signal from noise. We were able to figure out that beam loading the accelerator section makes such a configuration unstable and it would never turn on without significant input power. We introduced the alternative bi-resonant structure to disconnect the output klystron cavity coupled to the accelerator cells from the first cavities of the klystron part. We explained that new scheme would be less stable but would require significantly less input power, which made it our first choice to build a prototype.

We continued theoretical part with a brief theory of linear coupled oscillators describing resonantly coupled cavity behavior in the klystron and accelerator parts of a Klynac. We showed that even for complicated connections between different cells, eigen modes and eigen frequencies can be found in the process of a matrix diagonalization, which could be solved analytically for a low dimension matrix and computationally for an arbitrary amount of oscillators. Finally, we discussed how to minimize the impact of competing modes on Klynac behavior by minimizing a transit time factor for them in the coupling cavities.

In the third chapter we described how we designed a Klynac device, initially, for the type-1 structure where all cavities are coupled and then for the type-2 bi-resonant structure with two coupled circuits. We started our simulations for the klystron part in PIC code KLYNAC with uniform electric field in the cavities, optimized cavity positions and voltages while a phase shift between neighbors (coupled cavities were substituted by drifts) was fixed to π to maintain $\pi/2$ mode structure.

On the second step, we calculated field maps for the specific cavity geometries using Poisson Superfish and added them to our simulations. We obtained reduced efficiency for the klystron parts and performed additional adjustments on the cavity locations and voltage amplitudes to improve performance. We also used field maps for performing simulations in the accelerator sections.

We continued our design by describing the aperture realization in the PIC code and finding an optimum hole location and geometry to maintain a desired percentage of the electron beam going through. We discussed the accelerator section design and presented final outlines for both the type-1 and type-2 schemes.

Finally, we confirmed our theoretical estimate on the behavior of competing modes for the second type structure and discussed what would happen in that design if not enough input power was delivered to the system motivated by our experimental circumstances.

4.2 Possible applications

The work described in this thesis mostly concentrated on creating a proof-of-principle prototype for a Klynac-like compact accelerator rather than a specific device for particular applications. Here we will discuss what potential applications it can be used for and what limitations and requirements it would put on the system.

It does not look reasonable to have Klynac as an initial part of a high-energy accelerator, mostly because such an accelerator incorporates many klystrons, so the cost of one more klystron is not important. In addition a lot of high-energy accelerators, especially ones which are used for light sources, require a very good-quality electron beam. In opposite, low-energy accelerators (1-8 MeV), which are required to be as compact as possible, are the potential application range. Just as their high-energy counterparts, small-energy accelerators are often used for generating photons. When an electron decelerates, it produces radiation. This principle works for a klystron as well as for a Thompson scattering source. The mechanism is different every time, as well as energy scale, but the general idea remains the same: electron looses energy - photon gains it and vice versa, as it is realized in an accelerator, for instance. If an electron loses its energy slowing down in matter, it produces Bremsstrahlung radiation with spectrum reaching the electron energy (that is X or gamma rays). The last fact is one of the main reason for building low-energy accelerators.

Bremsstrahlung radiation can be used for nondestructive material testing. Hence, there are at least two potential areas where a Klynac device could be used: medicine and special nuclear materials (SNM) detection. Both require compact size, durability and low cost. For the medicine applications it might be required to put the whole structure on a gantry and move it around a patient. In this case, potential low Klynac weight (no klystron is required) would give a lot of benefits. The device might be driven by a low-power RF source ~ 2

kW, which is located remotely from the gantry as well as the source driving an electron gun. No complicated feedback system would be required to support stability and frequency synchronization between a klystron and accelerator.

For the SNM detection there are different levels for a system to be compact. First, one can locate the mobile unit on a truck; also, it could be carried in backpacks by a small group of two or three people. In the first case, Klynac might be realized as an amplifier with some RF input power device included. In the second case, one would have to find the way to realize it as an oscillator. In addition, compact electron gun probably driven by a mobile solid-state modulator has to be designed.

Finally, it will be very interesting to take a look on the electron beam phase space at the Klynac output and estimate what Thompson/Compton source could be created by back scattering the laser pulse from it [25, 26].

4.3 Future plans

Our nearest plans connected with Klynac is to finish the experimental setup for testing our prototype. Once all the problems are solved and all safety forms are signed, we will be able to measure the performance of the structure which has been built. The main goal will be to demonstrate acceleration and eventually validate the presented numerical simulations. If our input power is too low to drive our structure and we would have some experimental time, we would try to connect the pickup loop of the output accelerator cavity with a drive loop of the input klystron cavity and check if our device builds up any power from noise. The further work will depend on the experimental results of testing our prototype.

REFERENCES

[1] R. D. Ruth. An overview of collective effects in circular and linear accelerators. *Stanford Linear Accelerator Center*, Slac-PUB-4948, 1989.

[2] A.M. Sessler. Collective-effect accelerators and the challenge of attaining ultra-high energies. *Lawrence Berkeley National Laboratory*, LBL-15019, Sept. 1982.

[3] S. Corde et al. High-field plasma acceleration in a high-ionization-potential gas. *Nature Communications*, 7, doi:10.1038/ncomms11898, 2016.

[4] R. Wideroe. Uber ein neues Prinzip zur Herstellung hoher Spannungen *Arch. f. Elektrot*, 21, 387, 1928 (Wideroe's thesis in German).

[5] P. Waloschek. The infancy of particle accelerators: Life and Work of Rolf Wideroe. *DESY*, 2002.

[6] B. E. Carlsten, S. Russel. Microwave sources. *USPAS*, June 2012.

[7] J. C. Nygard. *U.S. Patent*, No. 2,922,921, 1960.

[8] R. F. Post. *U.S. Patent*, No. 2,940,001, 1960.

[9] Patent Rules, Consolidated. United States Patent and Trademark Office.

[10] S. Schriber. *Canadian Patent*, No. 1040309, 1978.

[11] J. L. Xie. A combined source of electron bunches and microwave power. *Review of Scientific Instruments*, doi: 10.1063/1.1623618, 2003

[12] J. M. Potter et al. The Klynac, an integrated klystron and linear accelerator. *AIP Conference Proceedings*, 1525, 178, 2013.

[13] E. A. Knapp. Design, construction, and testing of RF structures for a proton linear accelerator. *IEEE Trans. on Nucl. Sci.*, NS-12, 118, 1965

[14] D. A. Swenson et al. Stabilization of the drift tube linac by operation in the $\pi/2$ cavity mode. *Proc. 6th Int. Conf. on High Energy Accelerators, Cambridge, Mass.*, 167 (1967).

[15] HFSS (High Frequency Structure Simulator) Software. ANSYS Academic Research, Release 16.2

[16] G. Caryotakis The klystron: A microwave source of surprising range and endurance. *SLACPUB7731*, 1998.

[17] B. E. Carlsten et al. Mono- and bi-resonant Klynac. *Unpublished draft*, 2016.

[18] T. J. Kwan et al. Electron-beambreakup transit-time oscillator. *Phys.Rev.Lett.*, 66, 3221, 1991.

[19] W. B. Herrmannsfeldt. Egun - an electron optics and gun design program *Stanford Linear Accelerator Center*, Slac-331-28, 1988.

[20] A. Adelman et al. The OPAL Framework. Version 1.4.0. User's reference manual PSI, PSI-PR-08-02, 2016.

[21] A. Jensen et al. Developing sheet beam klystron simulation capability in AJDISK. *Stanford Linear Accelerator Center*, SLAC-PUB-15879, 2014.

[22] R. F. Holsinger. Reference manual. *Los Alamos Alamos National Laboratory*, LA-UR-87-126, 1987.

[23] S. O. Schriber. Effective shunt impedance comparison between S-band standing wave accelerators with on-axis and off-axis couplers, *Chalk River Nuclear Laboratory*, 1976.

[24] J. Sekutowicz. Cold- and beam test of the first prototypes of the Superstructure for the TESLA Collider *Stanford Linear Accelerator Center and DESY*,SLAC-PUB-10111, DESY-M-03-01T, 2003.

[25] A. Malyzhenkov et al. Optimization of Compton source performance through electron Beam Shaping, *Los Alamos Alamos National Laboratory*, LA-UR-16-28344, October, 2016.

[26] A. Malyzhenkov et al. Optimization of Compton source performance through electron beam shaping, *AIP Conference Proceedings*, 1812, 100008 (2017), March, 2017.